Chapter 4

APPLICATIONS OF SILICATE-MELT INCLUSIONS TO THE STUDY OF MAGMATIC VOLATILES

Jacob B. Lowenstern
U.S. Geological Survey, Mail Stop 910
345 Middlefield Road, Menlo Park, CA 94025

INTRODUCTION

Silicate-melt inclusions (MI) are small (~1 to 300 μm) blebs of silicate melt that are trapped within igneous phenocrysts (Fig. 1). They are glassy or crystalline, and are found within both extrusive and intrusive rocks. Because they can form at high pressures and are contained within relatively incompressible phenocryst hosts, they may retain high concentrations of volatile elements that normally escape from magmas during degassing. As such, analysis of these inclusions provides direct information on the volatile contents of magmatic systems.

A number of recent papers have used silicate MI to understand magma degassing, to characterize the compositions of immiscible fluids separating from magmas, and to study petrogenetic processes such as magma mixing and crystal fractionation. The use of MI has allowed greater understanding of igneous geochemistry and magmatic processes (Table 1). This paper reviews the nature and characteristics of silicate MI, the tools and methods for their analysis, and some important findings of recent studies.

Several previous reviews have also addressed the general topic of MI, and the interested reader is referred to these works. Clocchiatti (1975) reviewed optical and thermometric studies of MI in quartz and provided abundant observational and experimental data on the behavior of MI. Sobolev & Kostyuk (1975) synthesized the considerable volume of Russian literature on MI accumulated prior to 1975. Roedder (1979) gave a thorough discussion of silicate MI, their origins, and the methods of study and work to that date. Much of

Table 1. Data obtainable and not obtainable from silicate-melt inclusions

I. DATA OBTAINABLE FROM MI

1. Dissolved volatile concentrations in ore-forming and other magmas; H_2O, CO_2, Cl, S, F, B, Li and ore metals (See Table 2).
2. Minimum pressure of crystallization (*e.g.*, Anderson *et al.* 1989).
3. Approximate temperature during crystallization (See Roedder 1984).
4. Evidence for exsolved fluids during crystallization of phenocrysts (*e.g.*, Lowenstern 1994a).
5. Approximate (and partial) composition of coexisting exsolved fluids (*e.g.*, Anderson *et al.* 1989; Wallace & Gerlach 1994; Lowenstern 1994b).
6. Evidence for magma mixing (*e.g.*, Anderson 1976).
7. Composition of the melt phase in granites (Frezzotti 1992).
8. Time-scale of magmatism/volcanism (*e.g.*, Bogaard & Schirink 1994).

II. DATA NOT OBTAINABLE FROM MI

1. The composition of the bulk magma (*i.e.*, melt + phenocrysts + exsolved fluid).
2. Maximum pressure (depth) of entrapment.
3. Fate of fluids exsolved from the magma; mechanisms for fluid egress from magma.
4. Role of magma in formation of epithermal ore deposits (at least little direct information is available from silicate MI).

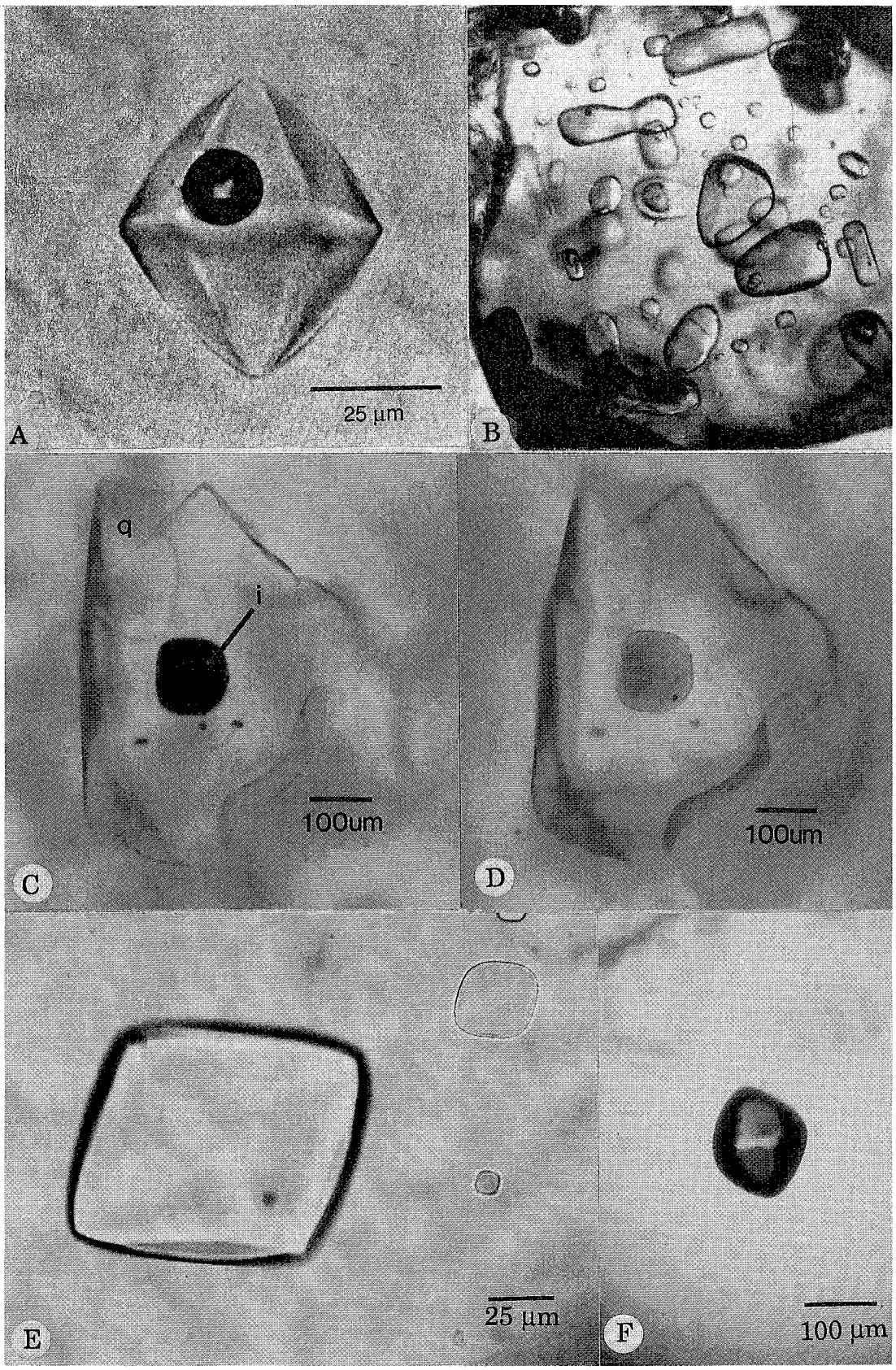
A
25 µm
B
q
i
C
100um
D
100um
E
25 µm
F
100 µm

this information is repeated in his later, more general volume on fluid inclusions (Roedder 1984). Roedder (1992) summarized evidence for immiscible fluids in the magmatic environment. Johnson *et al.* (1994) discussed MI, and the information they provide about the pre-eruptive volatile contents of four magmatic systems: Kilauea, Mt. St. Helens, the Bishop Tuff, and Mt. Pinatubo.

My review focusses on inclusions from andesitic to rhyolitic magmas, and concentrates on those studies with information useful to economic geologists and hydrothermal geochemists who seek understanding of fluids emanating from igneous systems. The review consists of two parts: it begins with a primer on the characteristics of MI and methods by which they can be studied, and the second half concentrates on recent studies and applications for petrologists and economic geologists.

THE FORMATION OF SILICATE-MELT INCLUSIONS

Types of Inclusions

The common terminology for categorizing aqueous or carbonic fluid inclusions becomes unwieldy when applied to silicate MI, particularly those in volcanic rocks. For example, most non-silicate fluid inclusions are described as: 1) *primary*, 2) *secondary*, and 3) *pseudosecondary* (Roedder 1984). *Primary* inclusions contain any phase present at the time of crystal growth. *Secondary* inclusions contain phases that enter crystals along fractures (after primary crystal growth has ceased) and then are trapped as the fractures heal. *Pseudosecondary* inclusions are also trapped along fractures, but before the crystal has ceased growing at its periphery. To most igneous petrologists, both primary and pseudo-secondary MI are "primary" in the sense that they are trapped within growing crystals and yield information on the composition of the silicate liquid during its evolution. Under some circumstances (such as magma mixing), there may be more than one primary melt from which the host crystal grew. It is difficult to envision how secondary MI may be trapped in volcanic phenocrysts (given the high viscosity of silicate melts), though Pasteris *et al.* (accepted) convincingly showed how non-silicate fluids can be trapped as secondary inclusions, particularly during fracturing events associated with magma ascent. Metasomatic secondary MI are commonly described in xenoliths found in volcanic ejecta (*e.g.*, Schiano *et al.* 1994) and can potentially form in plutonic environments if a silicate melt infiltrates a previously crystallized rock.

This review concerns itself with primary silicate MI, inasmuch as the term "primary" indicates that the crystals were still growing from silicate melt at the time the MI were trapped. Though most MI contain only one phase at the time of entrapment (silicate liquid), during cooling, that phase may unmix to form a vapor bubble and daughter crystals (Sorby 1858; Roedder 1984). Another class of inclusions that will be discussed is called *mixed* MI, which form by entrapment of more than one phase besides the silicate melt (Roedder 1984). The other phases may include microphenocrysts or *fluids*, with the latter used here to denote any volatile phase such as a low-density vapor or hypersaline liquid.

Entrapment Mechanisms

Roedder (1984: Chapter 2) and Sobolev &

Figure 1, (left). Transmitted-light photomicrographs of inclusions in quartz. (**A**) Silicate MI with negative crystal shape that reflects the bipyramidal habit of the host quartz. Note large (shrinkage?) bubble. From the Dolomite Mts., Italy (Clocchiatti 1975). (**B**) Multiple elongate silicate MI, most without bubbles, in quartz from Mont Dore (from Clocchiatti 1975). Field is 700 μm across. (**C**) Crystallized MI in quartz from Pantelleria (from Lowenstern & Mahood 1991). Letter 'q' shows quartz host, whereas 'i' denotes inclusion. (**D**) The same MI after heating the host quartz for several hours at 850 °C and atmospheric pressure. The inclusion is glassy and contains one very small bubble (arrow). (**E**) Three glassy, bubble-free MI of various sizes from Plinian fallout of the tuff of Pine Grove, Utah. (**F**) An empty inclusion (void) in quartz from the Plinian fallout of the tuff of Pine Grove. Such features are interpreted here to be leaked fluid inclusions that originally contained magmatic fluid/vapor, but no silicate melt. See text in section on Evidence for Trapped Fluids.

Kostyuk (1975) list a variety of mechanisms by which primary inclusions may form, including: 1) non-uniform supply of nutrients to the crystal face, resulting in skeletal growth, 2) undercooling, also resulting in skeletal growth, 3) formation of reentrants in the crystal during resorption events, followed by subsequent crystal growth, and 4) wetting by a separate immiscible phase (*e.g.*, molten sulfide or a vapor bubble) that creates irregularities in crystal growth, resulting in entrapment of that phase as well as the melt.

Though primary MI are found in nearly all volcanic rocks, they are not present within every individual crystal. Some crystals may contain scores of inclusions, implying that irregularities of phenocryst growth may control inclusion distribution. Figures 2a-c show secondary electron images of β-form quartz crystals from the

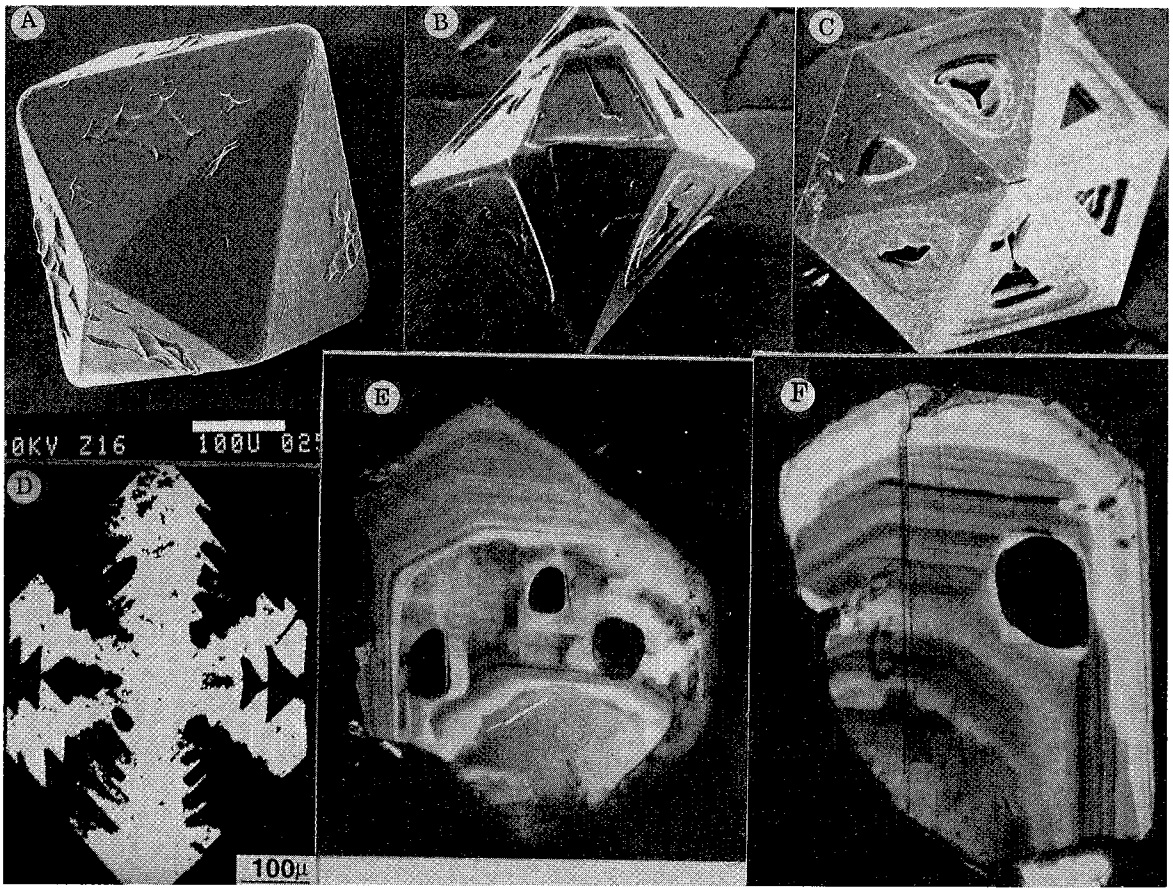

Figure 2. Photographs of quartz and feldspar crystals from silicic volcanic rocks demonstrate typical growth forms that trap MI. (**A**) Secondary electron image of a well-formed bipyramidal β-form quartz phenocryst from the 1912 eruption at the Valley of Ten Thousand Smokes, Alaska (from Lowenstern 1993). (**B** and **C**) Secondary electron images of quartz phenocrysts from the same eruption, displaying semi-skeletal growth in which interiors of crystal faces grow more slowly than edges. This results in gaps filled by silicate melt that may later be trapped as inclusions. Field in both photos is 1 mm across. From Clocchiatti (1975). (**D**) Transmitted-light photomicrograph of a section parallel to the *c* axis through the center of a quartz phenocryst from a liparite, showing skeletal growth pattern (adapted from Lemmlein 1930), as might be expected for crystals in preceding two photos. (**E** and **F**) Transmitted-light photomicrographs of plagioclase from pumice fallout deposited during the climactic eruption of Mt. Mazama/Crater Lake (from Bacon *et al.* 1992). The dark MI are along zonal arrays, just outside of patchy zones that may be formed during resorption events. In **E**, the elongate MI is 70 × 130 µm. In **F**, the MI is 90 × 120 µm.

high-silica rhyolite erupted in 1912 at the Valley of Ten Thousand Smokes, Alaska (Clocchiatti 1975). The images illustrate the common occurrence of 'gaps' or 'hoppers' in the bipyramidal faces. Comparison with a thin-section photomicrograph from Lemmlein (1930; Fig. 2d) illustrates how this common semi-skeletal growth phenomenon (MacLellan & Trembath 1991) could result in the formation of reentrants and hence form MI in volcanic quartz.

Plagioclase and pyroxene tend to trap MI in zonal arrays, permitting some studies on the sequence of inclusion formation. Bacon *et al.* (1992) studied MI in plagioclase and noted that large inclusions were commonly found adjacent to (outside of) areas of patchy zoning; these were interpreted to have formed during resorption (Figs. 2e, f). This arrangement seems to imply that, at least for plagioclase, resorbed crystal surfaces are favorable substrates for inclusion entrapment during subsequent growth events. Watson (1976) found that inclusion-rich zones correspond to sharp compositional gradients in the host plagioclase, implying that a considerable variation in either temperature or melt composition (*e.g.*, H_2O concentration), or both, enhanced crystal growth and inclusion entrapment.

Leaked or "Hourglass" Inclusions

Occasionally, the host crystal does not completely enclose the included melt, and the system remains open during cooling and decompression. As shown in Figure 3, such inclusions remain connected to the outside of the host by a narrow capillary filled with either silicate melt or a vapor phase. Hourglass inclusions fill the continuum between completely enclosed MI and reentrants in phenocrysts (Anderson 1991). By comparison of the various parts to Figure 3, it becomes apparent that petrographic examination of a sample in three dimensions is required to assess whether an MI was (or still is) an hourglass inclusion (*e.g.*, Figs. 3d, e). In addition, one can see that growth processes resulting in hourglass inclusions and reentrants can be confused with resorption textures.

Hourglass inclusions seem to form by the same sort of crystal-growth process that results in the gaps seen in Figures 2c and 2d. The capillary remains open if a pressure gradient keeps melt or vapor flowing through it during ascent of the magma (Anderson 1991). Because populations of these "leaked" inclusions may be variably degassed, they present a unique opportunity to constrain the timing and kinetics of gas exsolution during eruptive ascent. This was first recognized by Anderson (1991), who gave a detailed discussion of 'hourglass' inclusions and showed that they allow one to characterize the degassing and ascent history of quenched volcanic rocks. For other types of studies, however, hourglass inclusions should be avoided, as they do not retain volatile concentrations representative of the melt phase at the time of entrapment.

Does the Melt Inclusion Trap Representative Liquid?

One process of concern to researchers is the formation of boundary layers adjacent to growing crystals (Watson *et al.* 1982; Bacon 1989). Such layers can contain non-representative melt compositions because of the slow diffusion rates of incompatible melt components away from the crystal interface. If such a melt boundary-layer were trapped as an inclusion, it would provide misleading information about melt compositions.

Many studies have tried to assess the effect of boundary-layer phenomena. Most have noted the similar major-element compositions of MI and matrix glass and have concluded that the inclusions represent melt from which the crystals grew (Lowenstern & Mahood 1991; Dunbar & Hervig 1992b; Bacon *et al.* 1992). Sometimes, trace-element concentrations vary significantly between inclusions and associated matrix glass. For example, both Cl and Ti concentrations in melt inclusions from the Lower Bandelier Tuff vary by a factor of three (Dunbar & Hervig 1992a). The matrix glass contains lower amounts of Cl, yet higher Ti than do MI, a relationship inconsistent with entrapment of enriched boundary layers, which should contain higher concentrations of both elements. Lu *et al.* (1992) found that U and La were negatively correlated

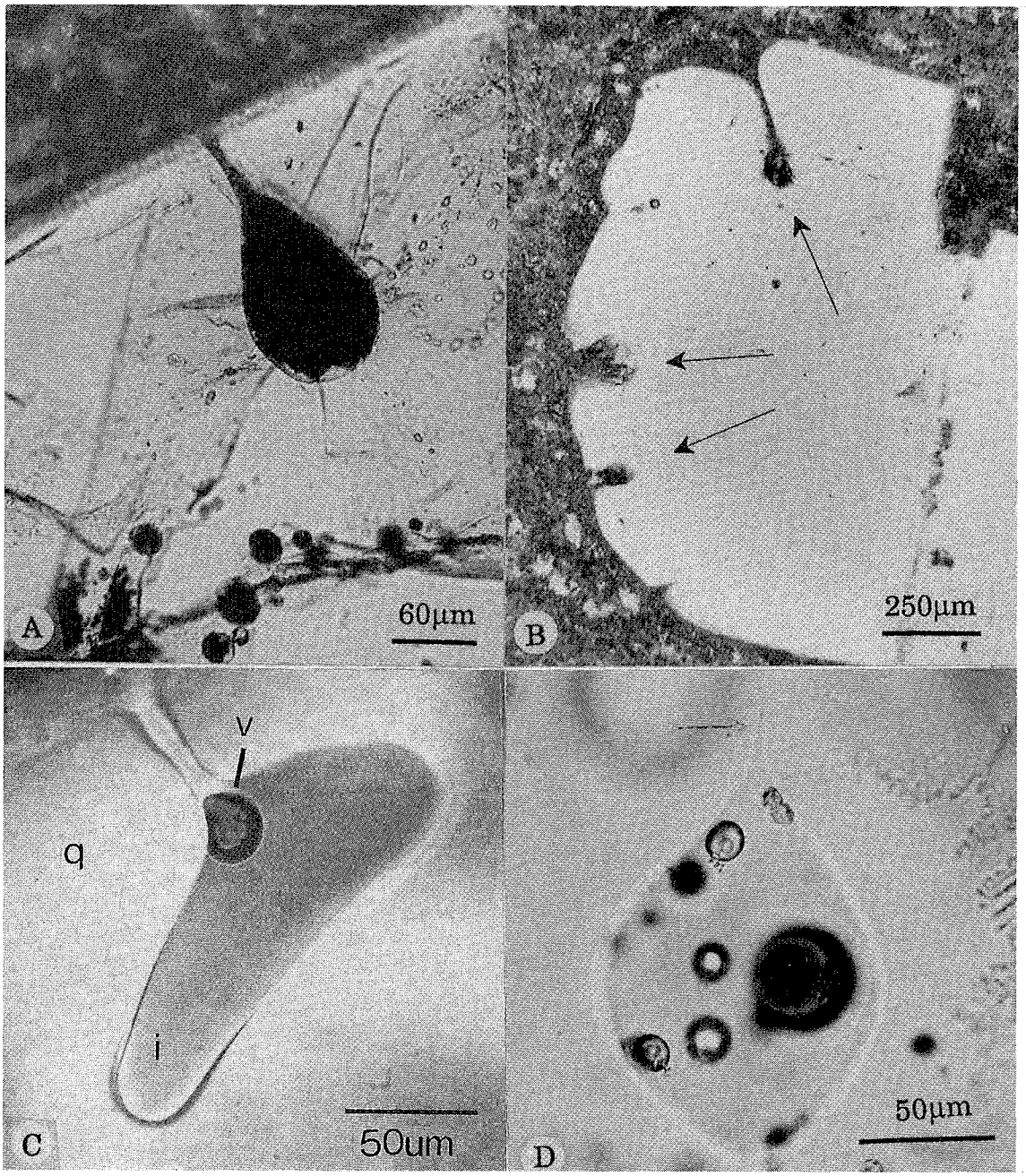

Figure 3. Transmitted-light photomicrographs of hourglass inclusions and reentrants in quartz. (**A**) Crystallized hourglass inclusion from the Pine Grove porphyry, Utah. Small capillary connects the bulk of the inclusion with the outside of the host crystal. (**B**) Hourglass inclusions form a continuum with simple reentrants, as illustrated by three hourglass/reentrants (arrows) in quartz grain from Pine Grove porphyry. (**C**) Glassy hourglass inclusion (i) in quartz (q) contains a large bubble (v) grown at inclusion end of capillary (from 1912 rhyolite erupted at Valley of 10,000 Smokes, Alaska; Lowenstern 1993). (**D**) A completely enclosed MI from the Pink Unit of the tuff of Pine Grove may have leaked prior to closure of the capillary (arrow), creating an inclusion with multiple bubbles. (**E top, page opposite**) Hourglass MI from the Valenza unit at Pantelleria (Lowenstern & Mahood 1991). Large bubble within remelted MI sits at end of long, thin capillary (arrows) that extends to crystal surface. Bright spots below bubble are other MI, out of focus beneath the inclusion of interest. Bright spot northeast of bubble is a refractory quartz bleb (Lowenstern 1994a).

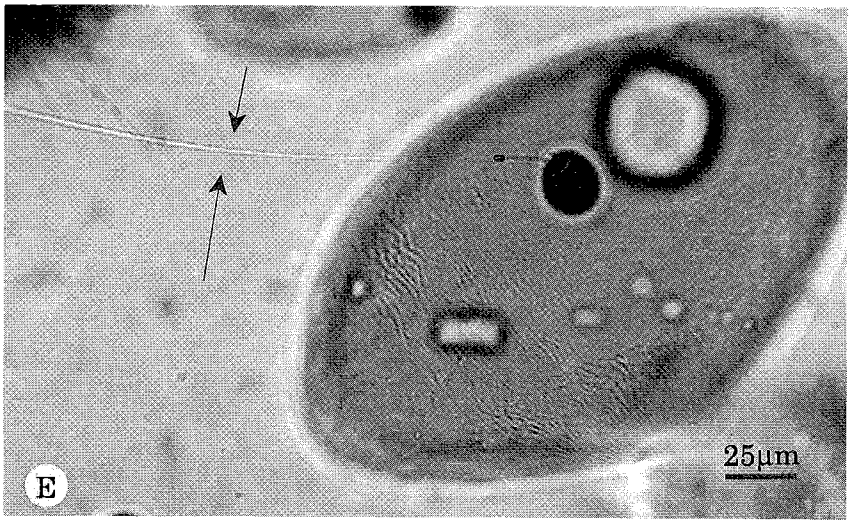

Figure 3E

within a group of quartz-hosted MI from the Bishop Tuff, consistent with crystal fractionation, but not enrichment in boundary layers (see also Anderson 1991). If immobile trace elements are not enriched in MI, it is unlikely that faster-diffusing species such as H_2O and CO_2 are greatly affected by boundary-layer phenomena. In summary, most workers have concluded that diffusion-related gradients such as boundary layers have little effect on analyzed populations of MI, and that the effects of boundary layers can be avoided by by studying inclusions larger than about 25 μm (Anderson 1974a).

CHANGES IN MELT INCLUSIONS AFTER ENTRAPMENT

Volumetric Behavior

Melt inclusions can be understood within the same theoretical and experimental framework that has been developed for other types of fluid inclusions (Hollister & Crawford 1982; Roedder 1984). Relative to silicate melt, quartz and most other magmatic phenocrysts are incompressible, so that after entrapment the inclusion volume is nearly constant (Roedder 1984). This means that the MI approximates an isochoric (constant volume) system with $\Delta P/\Delta T$ equal to the ratio of the coefficient of thermal expansion of the melt (α) to its compressibility (β) [~0.5 to 1.5 MPa/°C for typical silicic melt]. Because silicate melts are relatively incompressible, their isochores have relatively steep slopes, and the internal pressure of inclusions will change rapidly with relatively small changes in temperature (Fig. 4). As long as the quartz host is strong enough to withstand the pressure differential between the inclusion and external environment, the pressure in the MI will be a function of its temperature.

As a single-phase MI cools below its temperature of entrapment (T_t in Fig. 4), it will follow an isochore and depressurize until it becomes saturated with a volatile phase (*i.e.*, a 'shrinkage' bubble nucleates at T_b: Sorby 1858). Once the compressible bubble has formed, the inclusion will cool along the Melt/Vapor Curve until the supercooled silicate melt passes through the glass transition at T_g. Additionally, as the inclusion cools to room temperature, the internal pressure in the bubble may change as gases condense to their liquid state, and follow their own liquid/vapor curve. At 25 °C, a shrinkage bubble composed of pure H_2O should have an internal pressure equivalent to the vapor pressure of H_2O (3.2 kPa). A bubble in an inclusion of volatile-free melt should contain only silicate-melt vapor and thus should be a near-vacuum. Any bubble with a relatively high concentration of noncondensable gases (*e.g.*, CO_2) will retain higher internal pressure at 25 °C (up to ~6 MPa, the pressure at which liquid CO_2 forms). Water condensing from the cooling shrinkage bubble

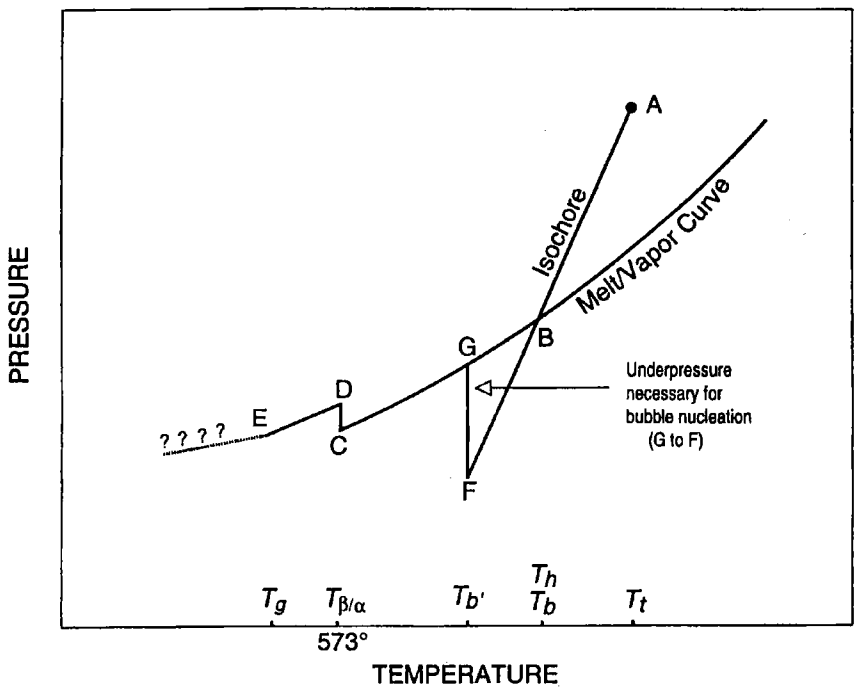

Figure 4. Schematic pressure–temperature trajectory for a silicate-melt inclusion in quartz. The inclusion traps vapor-undersaturated silicate melt (point A) at temperature T_t, and cools along its isochore until it reaches B. At this point, under equilibrium conditions, the melt should become saturated with a vapor phase and nucleate a bubble (at T_b). The inclusions would then cool along the melt/vapor curve to C. If cooled quickly, however, the inclusion may become supersaturated with respect to the vapor and will continue cooling along the original one-phase (melt) isochore, until the bubble finally nucleates at $T_{b'}$ (F). The internal pressure in the inclusion will then increase (F to G) until the inclusion returns to the melt/vapor curve. The inclusion follows this curve until $T_{\beta/\alpha}$, when the internal pressure in the inclusion increases due to the 1% volumetric contraction of the host. At T_g, the melt passes through the glass transition, and the bubble ceases to expand. If the inclusion were reheated in the laboratory, it would follow the path, E-D-C-G-B-A. T_h, the homogenization temperature, would occur at B. Figure adapted from Lowenstern (1994a).

may react with the inclusion glass, causing hydration at the bubble/glass interface (Anderson 1991).

Figure 5 shows the evolution of a crystallized melt inclusion as it is heated from room temperature up to 850 °C and then cooled. During heating, the inclusion progressively melts; the vapor bubble contracts until it disappears at T_h (850 °C). During cooling, a shrinkage bubble forms at $T_{b'}$ (710 °C), corresponding to point F in Figure 4. As in most systems, $T_{b'}$ is less than T_h because the inclusion must be significantly underpressured before it reaches saturation with the vapor bubble.

Other Origins of Bubbles

In principle, MI with similar origins should have similar vapor/melt ratios (see Anderson & Brown 1993). Typically, a single shrinkage bubble will constitute 0.2 to 5 vol.% of an inclusion, with the actual value dependent on cooling rate (Lowenstern 1994a), volatile content, and melt composition. If nearby MI have widely different vapor/glass ratios, other processes may have caused the bubbles to form.

Rapid decompression and resultant over-pressures within the inclusion, or even thermal shock, can result in fracturing of a phenocryst, depressurization, and vesiculation. In some circumstances, the fractures that cause this vesiculation may not be evident, as will commonly be the case in polished sections in which part or all of the fracture has been removed during sample preparation. For this reason, workers

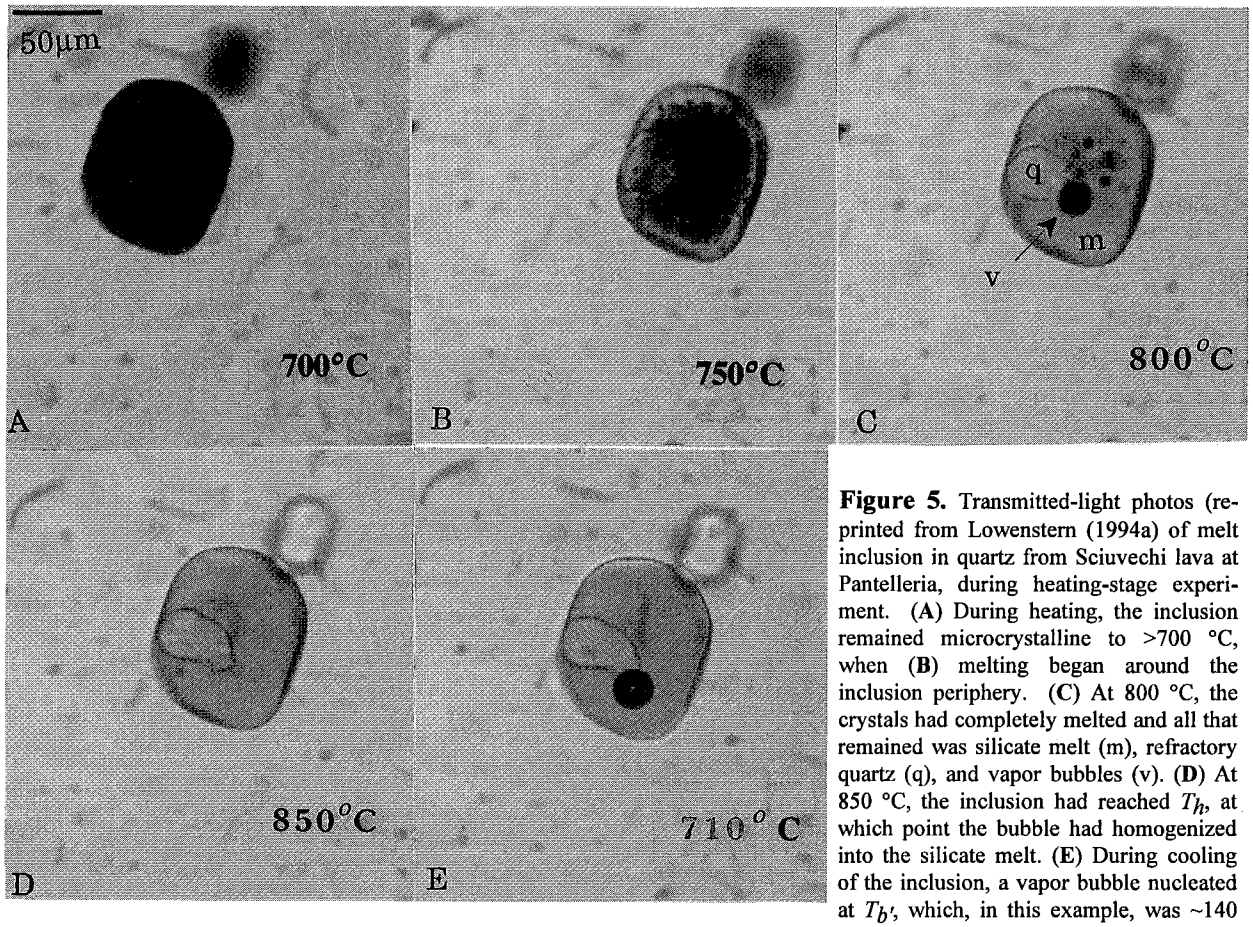

Figure 5. Transmitted-light photos (reprinted from Lowenstern (1994a) of melt inclusion in quartz from Sciuvechi lava at Pantelleria, during heating-stage experiment. (**A**) During heating, the inclusion remained microcrystalline to >700 °C, when (**B**) melting began around the inclusion periphery. (**C**) At 800 °C, the crystals had completely melted and all that remained was silicate melt (m), refractory quartz (q), and vapor bubbles (v). (**D**) At 850 °C, the inclusion had reached T_h, at which point the bubble had homogenized into the silicate melt. (**E**) During cooling of the inclusion, a vapor bubble nucleated at $T_{b'}$, which, in this example, was ~140 °C below T_h. Terminology as in Figure 4.

should consider avoiding inclusions with unusually large vapor/melt ratios, as these inclusions may have lost volatiles during fracturing events. Wallace & Gerlach (1994) and Pasteris *et al.* (accepted) concluded that most bubble-rich inclusions from the Pinatubo eruptive products had partly leaked.

Another cause for large vapor/melt ratios, however, is simultaneous entrapment of melt and a separate vapor or fluid phase (Roedder 1965; Belkin *et al.* 1985; Lowenstern *et al.* 1991; Frezzotti 1992; De Vivo & Frezzotti 1994). Such inclusions are particularly difficult to distinguish from leaked, bubble-rich inclusions. As a way of differentiating shrinkage bubbles from those primary vapors trapped as a separate phase, Belkin *et al.* (1985) recorded the behavior in a crushing stage. Shrinkage bubbles collapsed whereas the primary CO_2-bearing bubbles expanded when their host inclusions were opened to atmosphere. Lowenstern *et al.* (1991) and Lowenstern (1993) used an X-ray microprobe and infrared spectroscopy to analyze the compositions of bubbles within MI. The anomalous Cu and CO_2 contents of some bubbles were shown to be inconsistent with bubble formation by simple cooling/depressurization of an originally homogenous melt (or vesiculation during leakage). These results are discussed in greater detail below (section on Evidence for Fluid Saturation and Degassing). Another criterion for differentiating primary bubbles from those due to shrinkage is an unusually high homogenization temperature for the bubble (T_h) inasmuch as the inclusion must be taken to pressures greater than that of entrapment to dissolve the extra increment of vapor (Lowenstern 1994a). However, leaked inclusions also exhibit high T_h, and it is most prudent to assume that bubble-rich inclusions have formed due to leakage, unless there is compelling

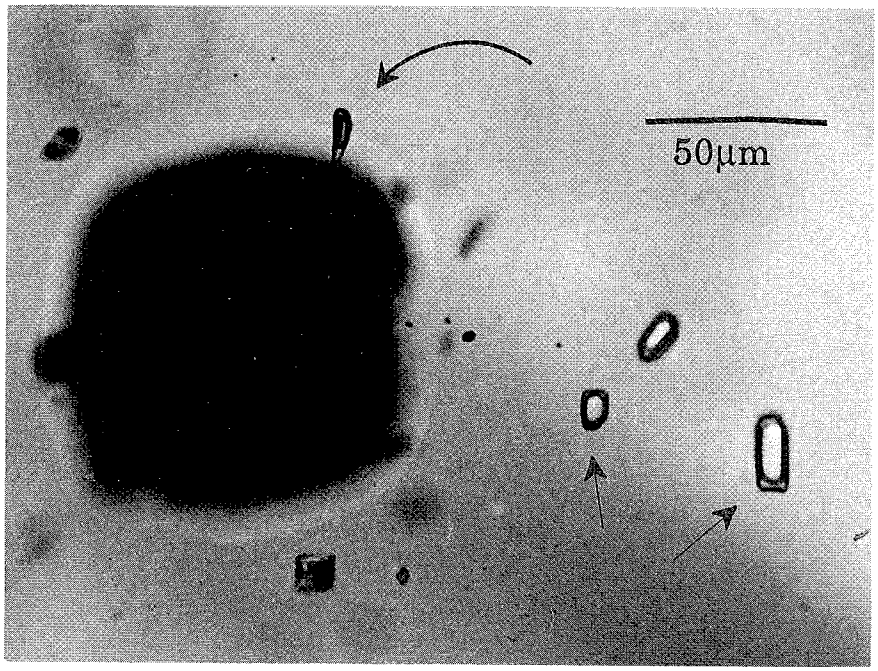

Figure 6. Large crystallized MI from upper unit of the tuff of Pine Grove, Utah. A group of coplanar, two-phase (vapor-dominated) fluid inclusions extends from the MI (two are indicated with straight arrows). One of the fluid inclusions (curved arrow) projects outward from the MI. The fluid inclusions are interpreted as forming along a fracture created when the inclusion decrepitated, prior to or during eruption. The inclusions appear to consist of vapor degassed from the inclusion at high temperature and pressure.

petrographic or chemical evidence to the contrary.

Decrepitation of MI

Figure 6 shows a group of vapor-rich fluid inclusions trapped along a fracture that formed by decrepitation of a silicate MI. Fractured and leaked MI are common in volcanic rocks. Some MI may decompress and decrepitate prior to cooling, during unloading of a magma chamber (Bacon *et al.* 1992; Tait 1992). During near-isothermal decompression, the pressure within an MI remains close to that at entrapment. This means that a large pressure gradient will exist between the inclusion and the crystal exterior, a situation that commonly results in cracking of the inclusion (Tait 1992). If cooling is rapid, however, one might expect a smaller pressure differential between MI and external environment, as the inclusion can decompress along its isochore (Fig. 4; point A to B). In fact, it seems that rapidly erupted rocks (i.e., Plinian deposits) have intact inclusions in comparison with inclusions in more slowly cooled lavas and pyroclastic flow deposits (Skirius *et al.* 1990; Dunbar & Hervig 1992a,b; Bacon *et al.* 1992). This correlates with the observation that MI in Plinian tephra tend to lack bubbles, whereas bubbles are common in co-erupted pyroclastic flows, which cool more slowly (Clocchiatti 1975; Skirius *et al.* 1990; Dunbar and Hervig 1992a; Lowenstern 1993). Because most MI become significantly volatile-supersaturated before nucleation of the shrinkage bubble occurs (Figs. 4 and 5; Lowenstern 1994a), inclusions may be underpressured by up to tens of MPa. As shown in Figure 4 (G to F), nucleation of a shrinkage bubble should cause a sharp increase in the internal pressure of an inclusion, and possibly cause cracking. MI in Plinian tephras may be quenched with sufficient speed that the bubbles are kinetically hindered from forming (Fig. 7; Lowenstern 1994a). In contrast, the lower cooling rates of lavas and pyroclastic flows allow bubble nucleation, resulting in an increase in the internal pressure of the inclusion and in decrepitation.

Crystallization

If allowed to cool slowly, MI will crystallize. Crystallized MI are typically described as 'devitrified', though it is not always apparent that the crystals grew from a glass rather than a still-molten liquid (in which case, the inclusions are not technically devitrified). Commonly, crystallization begins with precipitation of a host mineral on the inclusion wall. Under such circumstances, the original melt can be calculated from the compositions of MI hosted by different

phenocrysts formed from the same magma batch (Watson 1976; chapter 16 of Roedder 1984). Though many workers have concluded that MI compositions change little subsequent to entrapment (Beddoe-Stephens *et al.* 1983; Dunbar & Hervig 1992a,b; Bacon *et al.* 1992), other studies find evidence for limited post-entrapment crystallization of MI. Sisson & Layne (1993) reported that olivine-hosted MI from Fuego volcano were affected by post-entrapment crystallization (representing up to 11% of the inclusion mass). Webster & Duffield (1991) estimated that up to 15% of the mass of individual MI was precipitated onto the walls of their host quartz, depleting the glass in SiO_2. Presumably, such heterogeneous precipitation should not significantly exceed this value of 15% before the trapped melt becomes saturated with respect to the host phase, and crystallization stops. If other crystalline phases begin to form, crystallization of the entire melt can occur.

As with bubble size, the degree of crystallization seems to correlate to cooling rate (Fig. 7). Skirius *et al.* (1990) found that inclusions from slowly cooled pyroclastic flows commonly were crystallized, whereas those from more rapidly emplaced Plinian units remained glassy. Crystallized MI were remelted in the laboratory and quenched to form glassy inclusions that could be studied by microbeam methods (Skirius 1990; Skirius *et al.* 1990). In some systems, crystallized MI may be more pristine than glassy MI. Lowenstern & Mahood (1991) analyzed remelted pantellerite MI (*e.g.*, Figs. 1c,d; Fig. 5) for their H_2O concentrations and found that they were hydrous, whereas all originally glassy inclusions had low H_2O contents and seemed to have leaked. Presumably, the higher H_2O concentrations in intact inclusions increased ionic diffusivities and allowed crystallization, whereas the glassy inclusions, due to loss of water, were quenched as glass.

When kept at high temperatures, MI may change shape, regardless of whether they crystallize (Beddoe-Stephens *et al.* 1983). Evidently, the high temperatures permit redistribution of the host mineral, allowing surface energetics to control inclusion morphology. Skirius *et al.* (1990) noted that during prolonged heating experiments, originally rounded MI became more faceted, and the walls took on the shapes of negative crystals. Similar observations

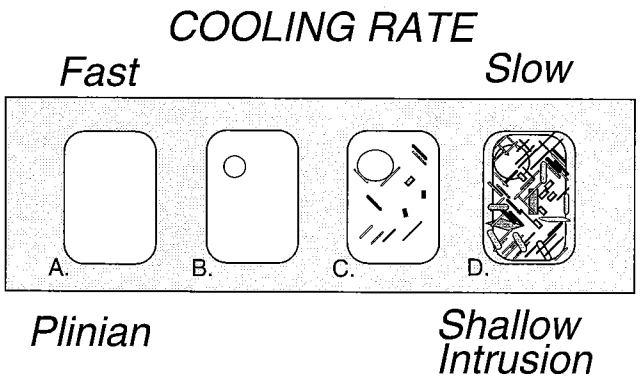

Figure 7. Schematic diagram of four crystal-hosted MI that undergo different cooling rates. (**A**) During rapid cooling, neither crystals nor bubble form prior to cooling to the glass transition. (**B**) A bubble may nucleate during less rapid cooling. (**C**) Diffusion during slow cooling allows the bubble to grow and the melt to partly crystallize. (**D**) Very slow cooling permits nearly full crystallization of the inclusion and growth of a layer of host mineral on the MI wall. Time-scales for bubble nucleation and crystallization are composition-dependent. Low-viscosity basaltic MI may fully crystallize within minutes, whereas more viscous rhyolitic MI may not crystallize even if kept at high (but sub-liquidus) temperature for years.

have been reported by Lowenstern (1994a) and Clocchiatti (1975) for both naturally and experimentally heated volcanic rocks, and by Frezzotti (1992) for partly crystallized MI in granites.

Diffusional Reequilibration

Fluid, mineral, and melt inclusions may not stay as closed systems over long time periods. Roedder (1984) suggested that the compositions of fluid inclusions in granulites may be affected by diffusion of H_2 and H_2O through the host minerals. This process has been confirmed experi- mentally and noted in other metamorphic and igneous rocks (Pasteris & Wanamaker 1988; Scowen *et al.* 1991; Hall *et al.* 1991; Mavrogenes & Bodnar 1994). Reequilibration seems enhanced by advection along microcracks and mineral defects, whose presence may be difficult to detect. These processes certainly will be important in slowly cooled granites, where melt inclusions, even if glassy, are kept at high temperatures for hundreds to thousands of years.

In molten systems, in which thermal and compositional gradients are lower, the effect of diffusional reequilibration will be lessened, but still may occur. Qin *et al.* (1992) provided analytical solutions to determine the effect of bulk diffusion on the H_2O contents of melt and fluid inclusions in quartz. They concluded that small inclusions (<25 μm) within a larger host quartz (1 mm diam.) can reach 95% reequilibration with the external environment in only two years. They suggested that bulk diffusion may have had an effect on the late-erupted Bishop Tuff pyroclastic flows, which contain lower H_2O concentrations than MI from Plinian units. However, experiments by Qin (1994) did not detect significant (and consistent) loss of H_2O from silicate MI during week-long experiments at high pressure and temperature. No other studies have been performed to assess the importance of this process for other (slower diffusing) chemical species. In general, the chemical gradients between inclusion and external melt may be insufficient for diffusion to affect MI compositions in shallow subvolcanic magmas.

Recent work by Bogaard & Schirnick (1994) seems to indicate that diffusional loss of components is negligible, at least for argon. These workers were able to date the time of entrapment of individual MI in quartz from the 0.76 Ma Bishop Tuff. The mean apparent age of MI from the basal fallout was 1.89 ± 0.03 Ma, and the group of analyzed inclusions defined an isochron of 1.93 ± 0.06 Ma. Inclusions from later-erupted pyroclastic flows gave an isochron of 2.3 ± 0.4 Ma. Apparently, the MI were trapped over a million years prior to venting of the system 760,000 years ago. The closure temperature for Ar diffusion through quartz is unknown, yet these data would seem to imply that it is greater than the magma temperature of the Bishop Tuff (~700 to 770 °C). Plausibly, the inclusions and their host quartz phenocrysts could have cooled to lower temperature within a supercooled glass or granite that was remobilized prior to eruption (though it is difficult to imagine all 500 km^3 of magma going through this process). Regardless of the mechanism, very little Ar apparently diffuses through quartz at near-magmatic temperatures.

TECHNIQUES FOR STUDY

Sample Preparation

Any study of MI should be preceded by a detailed field study of the host rocks. In addition, thin sections should be prepared for petrographic analysis of phenocryst phases, modes, rock textures, and phase relationships. Such information is vital to successful interpretation of data obtained through MI analysis.

Optimally, the MI-bearing phenocrysts should be picked from crystal separates. For pumiceous and scoriaceous rocks, such separates are particularly easy to prepare, as the matrix glass may be easily crushed and separated from crystals (often, by simply floating it away). Even for lavas and granites, crystals can be readily separated from groundmass and other phenocryst phases after crushing and use of heavy liquids. Any type of igneous phenocryst may contain MI. Olivine and quartz have been used for most studies because, in contrast to crystals with good cleavage, they tend to survive eruption and sample preparation without fracturing. An additional advantage of quartz is that its homogeneous and constant composition makes data acquisition and

reduction quite simple. Pyroxenes, though relatively opaque, also can be used successfully, and MI studies have used plagioclase, sanidine, leucite, apatite, and other phases.

Workers should avoid analysis of inclusions in grain mounts and thin sections if the MI were not observed and described prior to polishing. Instead, MI-bearing phenocrysts should be immersed in a mineral oil of appropriate refractive index to minimize scattering of light. Either a petrographic or stereoscopic microscope can be used to view the inclusions, or optimally, a spindle stage (*e.g.*, Anderson & Bodnar 1993). Such setups permit observation of the inclusion in three dimensions, allowing detection of cracks, capillaries, and other features that may indicate that the inclusion did not remain a closed system during cooling and depressurization (*e.g.*, Fig. 3). Workers should also record inclusion size, shape, and color, and describe any associated bubbles. Afterwards, the MI-bearing crystals can be mounted and polished.

Electron-microprobe Analysis (EPMA)

Most studies of MI will include major-element analysis by electron microprobe. This technique permits assessment of inclusion composition and heterogeneity, and can provide evidence for magma mixing and/or crystal fractionation. EPMA remains the most accurate technique for determining major elements, Cl, F, and S within inclusions. In the past, because of the difficulty in direct analysis of O, most samples have been analyzed and reported as oxides, with the mass of oxygen associated with elemental cations assigned during data reduction. If H_2O is present within a mineral or glass sample, this procedure results in reported totals of significantly less than 100% because the electron microprobe is not sensitive to the presence of H. This causes the amounts of both H and O to be under-reported. Anderson (1974b) used this deficit to his advantage in applying the "difference method" (100% minus EPMA analysis total) to estimate the dissolved-water concentrations of MI.

The difference method can be difficult to apply, however, because other factors can contribute to analysis totals less than 100%. Small, low-charge cations such as Na may migrate within the sample during electron-beam analysis, resulting in underestimates of actual abundances (Nielsen & Sigurdsson 1981). The problem increases for glasses, particularly if they are hydrated, and it becomes difficult to assess whether a low total is due to the presence of H_2O or reflects a poor analysis. Sodium migration can be minimized by using a low beam current, a large spot size, mean-atomic-number background corrections, and by counting Na at the beginning of the analysis. More sophisticated analytical protocols are discussed by Nielsen & Sigurdsson (1981).

Modern availability of synthetic spectrometer crystals permits direct analysis of O, so that the EPMA total for hydrous samples can be close to 100% (Nash 1992). Water concentrations can then be quantified by calculating the amount of oxygen not associated with the other major cationic species, and instead assigning it to H. Analytical uncertainties are similar to the "difference method", but the technique is preferable because it permits the analyst to be more confident that the calculated H_2O concentration is not spurious due to analytical problems such as elemental migration.

Ion Microprobe

Secondary Ion Mass Spectrometry (SIMS; *a.k.a.* ion microprobe) allows quantification of trace components within very small spots (<20 μm), with detection limits of <1 ppm for some elements. Several labs have used this technology to analyze silicate MI for a large variety of trace metals as well as the volatile elements F and H (Hervig *et al.* 1989; Lu *et al.* 1992; Sisson & Layne 1993; Webster & Duffield 1994). The greatest advantage of SIMS is that sample preparation is simple, involving only a singly polished section or grain mount that can be placed on different kinds of sample holders. If well-characterized standards are prepared that are similar to the samples in composition, and backgrounds are minimized, this technique can be both accurate and reproducible. Ihinger *et al.* (1994) gave a lengthy discussion of the use of SIMS for the analysis of H_2O and F in volcanic and synthetic glass.

Fourier Transform Infrared (FTIR) Spectroscopy

FTIR is a highly reproducible spectroscopic technique that can be used to quantify the amounts of dissolved H_2O and CO_2 in glass. Moreover, it provides information about the speciation of H_2O (molecular H_2O versus hydroxyl) and CO_2 (carbonate versus molecular CO_2) within the sample. Where calibrations have been performed, as for rhyolite and basalt, the technique is also highly accurate. For other compositions, accuracy is limited to about 20% relative. This technique remains the most reliable method for analysis of H_2O and CO_2 in MI, though sample preparation is tedious. The inclusion (within its host) must be prepared as a doubly polished wafer that sits upon an aperture through which a collimated (or focussed) beam of IR radiation is transmitted. Quantification requires knowledge of the sample thickness and density, as well as the absorption (extinction) coefficient ε, for the species of interest within the glass. Ihinger *et al.* (1994) give extinction coefficients for H_2O and CO_2 in a variety of glass compositions and review the pertinent literature on this technique.

Other Analytical Techniques

Although other techniques such as the X-ray microprobe (Lu *et al.* 1989) and Proton-induced X-ray Emission (Czamanske *et al.* 1993) have received less attention, they likely will increase the number of elements that can be analyzed in MI. These two techniques are relatively non-destructive (particularly the former) and can provide information on features beneath the sample surface (bubbles, crystals, *etc.*; Lowenstern *et al.* 1991). Quantification with the X-ray microprobe requires accurate knowledge of the sample thickness, and the concentration of at least one element within the sample (usually Fe or Ca). For most natural glasses, both techniques are most sensitive to elements with atomic number >20.

Other promising technologies include the nuclear microprobe (Mosbah *et al.* 1991), which has been used to analyze H in MI. Laser-ablation ICP mass spectrometry may also be used for trace-element analyses, though, as yet, no one has used this technique for analysis of glass inclusions.

Microanalytical dating procedures such as laser-based $^{40}Ar/^{39}Ar$ geochronology may be used to date individual MI. As discussed above, this technique has the potential to discern the timescale of magma-chamber processes (Bogaard & Schirnick 1994).

Heating Stage

Hundreds of studies have used a high-temperature heating stage to estimate entrapment temperatures of MI by noting the temperature of homogenization of shrinkage bubbles into the silicate melt (Sobolev & Kostyuk 1975). Ideally, homogenization indicates the minimum possible temperature of crystallization of the host phenocryst (Figs. 4, 5). The theory and methods associated with heating experiments are discussed by Roedder (1984) and Belkin (1994).

Beddoe-Stephens *et al.* (1983) found that heating-stage experiments gave homogenization temperatures too high to be consistent with magmatic temperatures inferred through other techniques, the difference presumably being due to kinetic factors (see also Lowenstern 1994a). Roedder (1984) described some of the difficulties in attaining useful data from heating-stage experiments. Measured homogenization temperatures may be highly dependent on the heating rate of the stage, as well as the viscosity of the silicate melt and diffusion rates of volatiles within the inclusion. In general, the faster the experiment is performed, the higher the apparent homogenization temperature because the diffusion rates for water and other volatiles are insufficient to allow the bubble to dissolve into the melt within the timeframe of the experiment.

Despite their inherent uncertainties, however, heating-stage experiments provide important constraints on magmatic temperatures (Li 1994), allow observation of magmatic fluids under magmatic conditions, and can be used to homogenize crystallized inclusions. Individual heating-stage assemblies are discussed in detail in Sobolev & Kostyuk (1975).

Data Interpretation

Once chemical and thermometric data have been collected, it remains necessary to ascertain which analyses contain useful data, and which

contain information not relevant to the scope of the study. For example, if the purpose of a study is to determine the pre-eruptive volatile concentration of a magma, data from leaked or fractured inclusions need to be discarded. Because fractures and capillaries may be difficult to detect, some inclusions may yield spurious data. Johnson *et al.* (1994) described three methods for MI data interpretation: the average approach, the high approach, and the one-by-one approach. In the average approach, all data are combined and the mean value is interpreted as the "correct" volatile concentration. When concerned about leaked inclusions, workers may reject low values and favor a high approach, wherein only the highest volatile concentrations are assumed to be correct. Alternatively, one can use a variety of criteria, including major-element composition, bubble size and geometry, inclusion texture, *etc.*, to choose those inclusions that are thought to yield the most reliable data. Though subjective, this one-by-one approach is more flexible, as each igneous rock will yield populations of MI that formed under different conditions and underwent different cooling and depressurization histories. Criteria for MI selection may differ with each new sample, and the inclusionist thus needs to observe carefully and to describe all inclusions prior to analysis.

CONCENTRATIONS OF DISSOLVED VOLATILES IN MI

One of the primary goals of most modern studies of MI has been to determine the amounts of dissolved volatiles present within crystallizing magmas. Most studies have concentrated on volcanic rocks, as they commonly are pristine and unaffected by post-entrapment phenomena such as leaking and crystallization. Table 2 lists studies that have determined the concentrations of dissolved volatiles in MI from silicic magmas such as dacites and rhyolites, compositions typically associated with hydrothermal ore-forming systems. Though not all silicic melts have been shown to contain high H_2O concentrations, most seem to have at least 4 wt.% dissolved H_2O in the melt. Some magmas are zoned in H_2O before eruption (Bishop and Bandelier Tuffs), whereas others are homogeneous (1912 Valley of 10,000 Smokes rhyolite, and Taupo). Carbon dioxide has been detected in several systems (Pine Grove, Bishop Tuff, Pinatubo), though others contain virtually none (Crater Lake, 1912 Valley of 10,000 Smokes rhyolite). Chlorine and F are highly variable in concentration, and their abundances seem to be correlative with tectonic setting (higher Cl/F in arcs relative to continental settings). Sulfur is generally very low (<100 ppm) in high-silica rhyolitic melts with < 1.0 wt.% FeO, although there is experimental evidence that oxidized, high-temperature silicic melts can contain higher concentrations of S as dissolved sulfate (Luhr 1990). Table 3 summarizes current understanding of volatile concentrations in silicic melts, based on analyses of silicate MI.

Data on magmatic volatiles have the following four applications: (1) they provide constraints on the amounts of magma-derived volatiles likely in ore-forming systems and on the general compositions of exsolving fluids. (2) They can demonstrate the relative importance of decompression-related degassing versus crystallization-induced degassing on the fluid-release history of a magma (Lowenstern 1994b). For example, if a magma is shown to have been volatile-saturated at a given depth, the mass of exsolved fluid produced during further ascent can be calculated (Shinohara & Kazahaya this volume). (3) They give reliable estimates of the dissolved concentrations of oremetals in magmas prior to degassing. Prior to the study of MI, economic geologists had to depend solely on analyses of degassed intrusions and extrusive rocks to characterize the metal and volatile composition of potential ore-forming magmas. (4) They may be used as geobarometers to determine the minimum pressures at which crystals grew (Anderson *et al.* 1989; Lowenstern 1994b).

Care must be used when interpreting data from MI, as they represent only a single phase within the magma reservoir: the melt phase. To estimate the total amount of volatiles in a magma reservoir, one must have constraints on the relative amount of melt, crystals, and exsolved fluid (Gerlach *et al.*, accepted; Wallace *et al.* 1994). Though MI yield constraints on the

Table 2. Volatile concentrations in a variety of recently studied silicic magmas, as determined by analysis of silicate MI

Unit	REFERENCE	SiO_2 in melt (wt.%)	H_2O (wt.%)	F (wt.%)	Cl (wt.%)	S (ppm)	CO_2 (ppm#)
Taupo Volcanic Zone, NZ							
Taupo, 2 ka	Dunbar *et al.* (1989)	73	4.3	0.045	0.17	<200	-
Hatepe, 2 ka	"	76	4.3	0.043	0.17	<200	-
Okaia, ~22 ka	"	-	5.9	0.047	0.21	<200	-
Pine Grove, USA- 22Ma	Lowenstern (1994b)	77	6.0-8.0	0.358	0.62	<60	up to 970
Taylor Creek, NM USA	Webster & Duffield (1994)	70	<2.0	0.15-3.9	0.23-0.37	-	-
Galeras, Col. 1991-92	Stix *et al.* (1993)	-		0.02-0.1	0.09-0.25	50	-
Toba, Indonesia 75ka	Newman & Chesner (1989)	76	5.2-5.7	-	-	-	<100
Santa Maria 1902	Palais & Sigurdsson (1989)	69	-	-	0.139	200	-
Santa Maria 1902	Roggensack *et al.*(1993, &†)	73	4.2		0.13	300	
Mt. St. Helens 1530	Palais & Sigurdsson (1989)	71	-	-	0.077	70	-
Mt. St. Helens 1980	Rutherford *et al.* (1985)	73.5	4.6±1.0	-	0.10±0.03	100±100	-
Nevado del Ruiz 1985	Layne *et al.* (1992)	70-74	1.6-3.3	0.05-0.14	0.01-0.18	-	-
Lower Bandelier Tuff	Dunbar & Hervig (1992a)						
Plinian	"	76-77	4.0-5.5	0.2-0.3	0.2-0.25	-	-
Basal Ignimbrite	"	76-77	3.0-4.0	0.1-0.2	0.15-0.25	-	-
Main body Ignimbrite	"	76-77	2.0-3.0	0.05-0.15	0.1-0.25	-	-
Katmai, AK USA 1912 Rhyolite	Lowenstern (1993)	77	3.4-4.2	-	-	-	<50
Katmai, AK USA 1912	Westrich *et al.* (1991)						
Rhyolite	"	77	3.8	0.063	0.193	<65	-
Dacite	"	77	2.3	0.064	0.179	120	-
Andesite	"	74	1.0	0.053	0.169	170	-
Crater Lake, OR, USA	Bacon *et al.* (1992)						
Climactic: 6450 ybp	"	73	3.9	0.04	0.188	-	<25
Cleetwood Flow, OR	"		5.3	0.03-0.05	0.09-0.14	-	<25
Llao Rock, OR	"		3.8-4.7	0.03-0.07	0.18-0.21	-	<25
Mt. Pinatubo Phillip.	Wallace & Gerlach (1994)	75-78	6.0-6.5	-	-	60 -90	280-415
June 15, 1991	Gerlach *et al.* (accepted)	75.6	<6.6	-	0.088	60-120	
Bishop tuff, CA USA (740 ka)							
Plinian	Anderson *et al.* (1989)	77	5.1-6.8	-	0.08	-	up to 190
Early ignimbrites	Skirius *et al.* (1990)	77	5.0-6.9	-	-	-	up to 213
Mono lobe ignimbrite	"	77	3.6-4.5	-	-	-	up to 660
Plinian	Dunbar & Hervig (1992b)	77	3.5-6.0	0.05	0.07	-	-
ignimbrites	"	77	2.0-4.0	0.05	0.07	-	-
Plinian	Wallace *et al.* (1994)	77	6.0±0.4	-	-	-	60±40
Early ignimbrite	"	77	6.5±0.3	-	-	-	120±60
Mono Lobe ignimbrite	"	77	4.6±0.4	-	-	-	150-1100
Juniper Mtn. Volcanic Center, ID, USA	Manley (1994)						
Badlands (lava)	"	75	1.4-3.8	0.09-0.23	0.06-0.11	-	-
Badlands (sub-Plinian)	"	77	1.7-3.6	0.12-0.17	0.08-0.13	-	-
Carter Spring (lava)	"	76	1.4-3.1	0.14-0.51	0.08-0.13	-	-
" " (fountain-fed)	"	77	0.6-2.1	0.12-0.21	-	-	-
Peralkaline Rhyolites							
Pantelleria, Italy	Lowenstern & Mahood (1991)	70*	1.4-2.1	-	~0.9	-	<100
Pantelleria, Italy	Kovalenko *et al.* (1994)	69-70*	up to 4.3%	0.10-0.26	0.60-1.20	-	-
Fantale, Ethiopia	Webster *et al.* (1993)	71*	4.6-4.9	0.30	0.30	-	-
Olkaria, Kenya	Wilding *et al.* (1993)	~70*	0-3.3%	-	-	-	-

Note: Data presented as X000 -Y000 indicates range of values in original publication. Data presented with '±' shows 1σ as listed in original publication. Dash indicates data not reported.

CO_2 by IR spectroscopy (FTIR). In studies with CO_2 data, H_2O data are also by FTIR.

† Personal communication (1994)

* Peralkaline rocks: Molar $(Na_2O+K_2O)/ Al_2O_3 >> 1.0$

Table 3. Summary of recent studies of volatile concentrations and saturation pressures in unleaked MI from high-silica rhyolites

Volatile Species	Typical Concentrations	Additional Information
H_2O	Rarely < 3% and rarely > 7%	Lower concentrations common in leaked MI
CO_2	Up to 1000 ppm, though some systems contain very little (<25 ppm)	Concentration highly dependent on degree of pre-entrapment degassing
Cl	600 ppm to 2700 ppm	Peralkaline rhyolitic and some mafic MI contain >3000 ppm
F	400 ppm to 1500 ppm	Continental systems may contain much higher concentrations: >1 wt.%
S	Usually < 200 ppm: often < 60 ppm	Concentrations are much higher in andesites and basalts
Saturation Pressure	Generally between 1 and 4 kb	Calculated as minimum pressure at which MI was trapped, given H_2O and CO_2 concentrations

composition of fluids in equilibrium with the magma, one must also recognize that the composition of exsolved fluid may change as it ascends from the magma, and cools and interacts with the surrounding environment (Hedenquist this volume).

EVIDENCE FOR FLUID-SATURATION AND DEGASSING

One of the important conclusions from several studies of MI has been that silicic magmas commonly are saturated with a free fluid (volatile) phase prior to eruption. Three primary lines of evidence from MI have supported this conclusion: 1) mass-balance constraints, 2) buffering of dissolved volatile concentrations, and 3) inclusions of non-silicate fluids such as vapors and hypersaline melts.

Mass-balance Constraints

Commonly, volcanologists have estimated volatile fluxes during eruptions by determining the difference in the concentrations of elements such as Cl and S in early-formed MI and the outgassed matrix glass adhering to the outside of erupted phenocrysts (*e.g.*, Palais & Sigurdsson 1989). This technique (commonly called the 'petrologic method') implicitly assumes that the only source of volatiles is from degassing silicate melt, and that all volatiles are dissolved in the melt at the time of MI entrapment. Combined with an estimate for the volume of erupted magma, this allows calculation of the mass of volatiles released from degassing melt. The development of satellite-based monitors of atmospheric chemistry permits an independent (and more direct) means of estimating volcanic gas flux (Symonds *et al.* 1994). During the 1991 eruption of Mt. Pinatubo, Philippines, satellites recorded a S flux orders of magnitude greater than that predicted by analysis of MI. Westrich & Gerlach (1992) found that the S concentrations in MI from Pinatubo were nearly identical to those in outgassed matrix, and that only a trivial amount of the erupted S could be attributed to degassing of melt subsequent to MI entrapment. They concluded that accumulated vapor accounted for most of the erupted S and estimated that it composed 2 to 5 vol.% of the magma at the time the MI were trapped. Other potential S sources, such as geothermal fluids, S-bearing crystals, and unerupted magma, were assessed as unlikely (also see Wallace & Gerlach 1994; Gerlach *et al.*, accepted). Similar findings were reported for Redoubt Volcano in Alaska, and Mt. St. Helens, Washington (Gerlach *et al.* 1994; Gerlach & McGee 1994). The studies of Gerlach and

colleagues highlight the fact that MI provide direct information on the melt phase, but not on the entire magma (Table 1; item II.1).

Fluid Solubility and Buffering Paths

The concentrations of volatiles in MI can be used to estimate the depth at which fluid should exsolve from a magma, and to estimate the composition of the evolved fluid. A saturation pressure is the minimum pressure at which a melt could have been trapped without being fluid-saturated. Saturation pressure can be calculated by incorporating volatile solubility models for the composition of interest as a function of temperature and pressure (Holloway & Blank 1994). Figure 8 illustrates the use of MI to gain insight into an ore-bearing system, the Pine Grove porphyry Mo system in Utah (Lowenstern 1994b). Extrusive rhyolites were used as a proxy for coeval and comagmatic porphyries that host high-grade MoS_2 ore (Keith *et al.* 1986). Lowenstern (1994b) analyzed thirty MI (black dots) for CO_2 and H_2O by FTIR spectroscopy. Isobars represent the range of compositions of melts in equilibrium with H_2O-CO_2 fluids at a given pressure. For each isobar, the mole fraction (X) of H_2O in the fluid phase decreases from one (H_2O saturation) on the x axis to zero (CO_2 saturation) on the y axis (as H_2O and CO_2 are completely miscible under these conditions). As indicated in Figure 8, all analyzed melts would be saturated with fluid if allowed to ascend to pressures less than ~250 MPa, and several would have been fluid-saturated at pressures >400 MPa. The data set was explained by entrapment of inclusions during decompression degassing, wherein H_2O and CO_2 vary due to partitioning of volatiles from melt to vapor during magma ascent. The high saturation pressures implied that the Tuff of Pine Grove began degassing at ~16 km depth (430 MPa), about 12

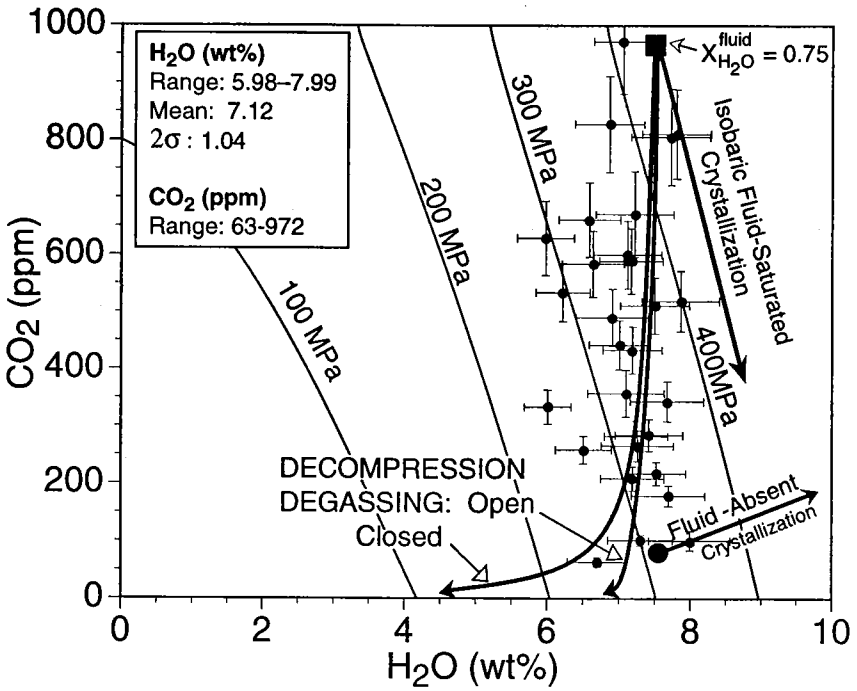

Figure 8. Solubility plot for the system H_2O-CO_2-rhyolite at 675 °C. Small filled circles (with 2σ errors) denote compositions of analyzed melt inclusions from Plinian unit of tuff of Pine Grove (Lowenstern 1994b). Lines labelled in units of pressure (MPa) show isobaric solubility of H_2O and CO_2 as a function of fluid composition – their intersections with the y and x axes give CO_2 and H_2O solubility, respectively, all other points being mixtures (isopleths not plotted). Labelled trends display the effects of open and closed-system decompressional degassing, and isobaric fluid-saturated degassing (starting from the filled square), as well as fluid-absent crystallization (at P >440 MPa: ~16 km lithostatic) starting from the large filled circle. Data are most consistent with entrapment of MI along a degassing trend, during ascent of the magma, prior to eruption. Figure from Lowenstern (1994b).

km below the depth at which the associated porphyries were emplaced. The magma therefore must have been quite vesicular by the time it reached the level of porphyry emplacement (20 to 40% vesicularity). Lowenstern (1994b) suggested that the decrease in magma density and increase in porosity associated with ascent and degassing are critical elements of the mineralizing process in porphyry Mo systems (see also Shinohara & Kazahaya, this volume). Moreover, the low Mo (<5 ppm) and high H_2O and CO_2 concentrations in the MI were used as evidence that porphyry Mo deposits are not formed by shallow, crystallization-induced degassing of metal-rich magmas, but are formed by streaming of exsolved volatiles from a deep chamber of more normal magma (Lowenstern 1994b; Keith & Shanks 1988).

Saturation plots such as Figure 8 were first used by Anderson *et al.* (1989) and Skirius (1990), who measured H_2O and CO_2 concentrations in MI from the Bishop Tuff and found that their compositions were consistent with isobaric, vapor-saturated crystallization prior to eruption (similar trend shown on Fig. 8). Wallace *et al.* (1994) plotted CO_2 versus the incompatible element U to calculate the amount of isobaric fluid-saturated crystallization prior to eruption of the Bishop Tuff. This allowed them to estimate the mass of exsolved fluid in the pre-eruptive magma chamber. For the 1991 Pinatubo eruption, Wallace & Gerlach (1994) analyzed MI and found that the amounts of dissolved H_2O and CO_2 were sufficiently high that the magma had to crystallize at pressures $\geq$ 250 MPa. This pressure agrees with that estimated for the Pinatubo magma reservoir by a variety of experimental, geophysical, and mineralogical criteria (Gerlach *et al.*, accepted).

Besides H_2O and CO_2, other volatiles have been used as evidence for saturation with a fluid phase. Lowenstern (1993) analyzed MI and matrix glass from the 1912 eruption at the Valley of 10,000 Smokes and found that Cl, S, and Cu apparently had their concentrations buffered by non-crystalline phases (*i.e.*, exsolved fluid). Metrich & Clocchiatti (1989) found evidence for two-stage degassing of the magma erupted in 1763 at Etna volcano in Sicily: an earlier degassing stage recorded in the variant compositions of silicate MI, and a later one that resulted in loss of S (though little Cl) from the bulk rocks during eruption. Stix *et al.* (1993) showed that MI compositions recorded a loss of H_2O, S, and Cl during shallow degassing of magma from Galeras Volcano in Colombia. The degassing was accompanied by continued crystallization of the magma, and by fluid release into a confined space and the resulting explosive activity observed from 1988 to 1993.

Sometimes, the fluid phase can unmix to form two fluids in equilibrium with the melt phase (*e.g.*, vapor and hypersaline liquid for the NaCl-H_2O system). This can cause the concentration of Cl to be fixed for a given pressure and temperature (Shinohara 1994; Candela & Piccoli this volume). Layne & Stix (1991) noted that the concentrations of Cl in melt inclusions could be used to deduce which lavas from the Valles caldera had been saturated with both a vapor and hypersaline brine. Similarly, Lowenstern (1994a) observed that peralkaline rhyolites (pantellerites) from Pantelleria, Italy, have melt Cl concentrations consistent with saturation with both vapor and a hypersaline phase.

Trapped Vapors and Hypersaline Liquids

Melt inclusions also yield direct evidence about fluids in magmatic systems. Mixed inclusions may contain any combination of immiscible phases present at the time of crystal growth. Along with silicate melt, these inclusions may contain sulfide and hypersaline liquids, vapor, or other crystals. Some criteria for identifying mixed inclusions are introduced above (subsection on Other Origins of Bubbles). If the different phases can be identified and differentiated, they can provide direct information on the compositions of immiscible phases within the magmatic system. Roedder (1992) gave a lengthy discussion of the significance of immiscibility in magmatic systems, and reviewed recent works that describe mixed inclusions in volcanic and intrusive rocks.

Primarily two kinds of non-silicate magmatic fluid are found in mixed MI: hypersaline liquid (>~40 wt.% NaCl equiv.) and low-density, low-salinity vapors. Roedder & Coombs (1967) and Roedder (1972) found the former in granitic

nodules ejected during eruptions of peralkaline trachytes from Ascension Island. More recently, several authors have described salt clusters in MI within quartz and feldspar from the peralkaline rhyolites from Pantelleria, Italy. When heated to magmatic temperatures, these clusters melt to form hydrosaline liquid that is immiscible with the silicate melt (Clocchiatti *et al.* 1990; Solovova *et al.* 1991; Lowenstern 1994a) and coexisting vapor (Solovova *et al.* 1991; Lowenstern 1994a). Remnants of the hypersaline fluid were found in outgassed matrix glass (Kovalenko *et al.* 1993; Lowenstern 1994a). De Vivo & Frezzotti (1994) summarized the evidence for immiscible fluid phases in Italian subvolcanic systems, and discussed the significance of the phases.

Other workers have discovered evidence for entrapment of mixed inclusions of vapor and silicate melt. Roedder (1965) described CO_2-rich bubbles (with liquid CO_2 at room temperature) coexisting with basaltic glass in melt inclusions from phenocrysts in basalts (19 different localities) and their associated ultramafic xenoliths (72 localities). Densities of these inclusions indicated entrapment at depths from 10 to 15 km. Frezzotti *et al.* (1991) corroborated the work of Metrich & Clocchiatti (1989; described above) by finding two generations of CO_2-rich vapors trapped along with silicate melt in mixed inclusions within phenocrysts as well as ejected ultramafic xenoliths. Similar mixed inclusions of vapor and silicate melt have been described in silicic systems. Pasteris *et al.* (accepted) used Raman spectroscopy to study vapor bubbles in MI from Pinatubo that contained high CO_2 pressures. The bubbles were too CO_2-rich to have formed during cooling and shrinkage of the MI, and the authors concluded that the inclusions trapped both silicate melt and an immiscible CO_2-bearing vapor. Subsequent to entrapment, the inclusions partly leaked, but still retained significant CO_2.

Immiscible fluids trapped in MI can contain evidence for the volatility of ore-forming metals in magmatic systems (see also Candela & Piccoli this volume; Bodnar this volume). Figures 9A and B show an MI that is thought to have formed as a two-phase mixed inclusion (melt + fluid) within a quartz phenocryst of peralkaline rhyolite (Lowenstern *et al.* 1991). The inclusion contained a large bubble with abundant Cu, S, and Cl mineralization on its wall (Figs. 9C, D). Only a minority of MI from these rhyolites contained the Cu-rich bubbles. Using infrared spectroscopy on the same samples, Aines *et al.* (1990) found that large, Cu-bearing bubbles contained CO_2 anomalies. Both studies concluded that the anomalous CO_2 and Cu in some samples were due to coeval entrapment of silicate melt and coexisting Cu-bearing fluid. Plausibly, the Cu could have come from a small droplet of immiscible hydrosaline liquid (Lowenstern 1994a) trapped along with a CO_2-bearing vapor bubble in the MI. For the 1912 eruption at the Valley of 10,000 Smokes, Lowenstern (1993) also concluded that MI with large Cu-bearing bubbles represented mixed inclusions of exsolved fluid and melt. He used the concentration of Cu in the bubbles and coexisting glass to estimate fluid/melt partition coefficients.

The origins of some inclusions have proved more difficult to explain. Naumov *et al.* (1991) described rhyolites with quartz crystals containing presumed coeval melt and fluid inclusions. The fluid inclusions were dense (specific gravity = ~0.9) and H_2O-dominated, implying extremely high entrapment pressures (>600 MPa) if the inclusions were trapped at magmatic temperatures. The silicate MI contained only 3 or 4 wt.% H_2O, only one-third of that expected for a silicic melt saturated with a H_2O-rich phase at >600 MPa. Figure 1F shows another puzzling inclusion type found in quartz from intrusive and extrusive units of the Pine Grove system of Utah (Keith *et al.* 1986). These 'empty' inclusions are located within the same growth zones as MI, are not intersected by capillaries or fractures, yet contain no detectable gas, liquid H_2O, or mineralization other than minor Fe- and Ca-bearing minerals along the inclusion walls (J.B. Lowenstern, unpublished). Because they are so different from hourglass inclusions from the same deposit (they contain NO glass or crystallized melt), they do not seem to have formed from leakage of silicate MI. Though they lack obvious fractures or capillaries, they are interpreted to be leaked inclusions of magmatic fluid. Gutmann (1974) found similar tubular voids in labradorite phenocrysts from Sonora, Mexico.

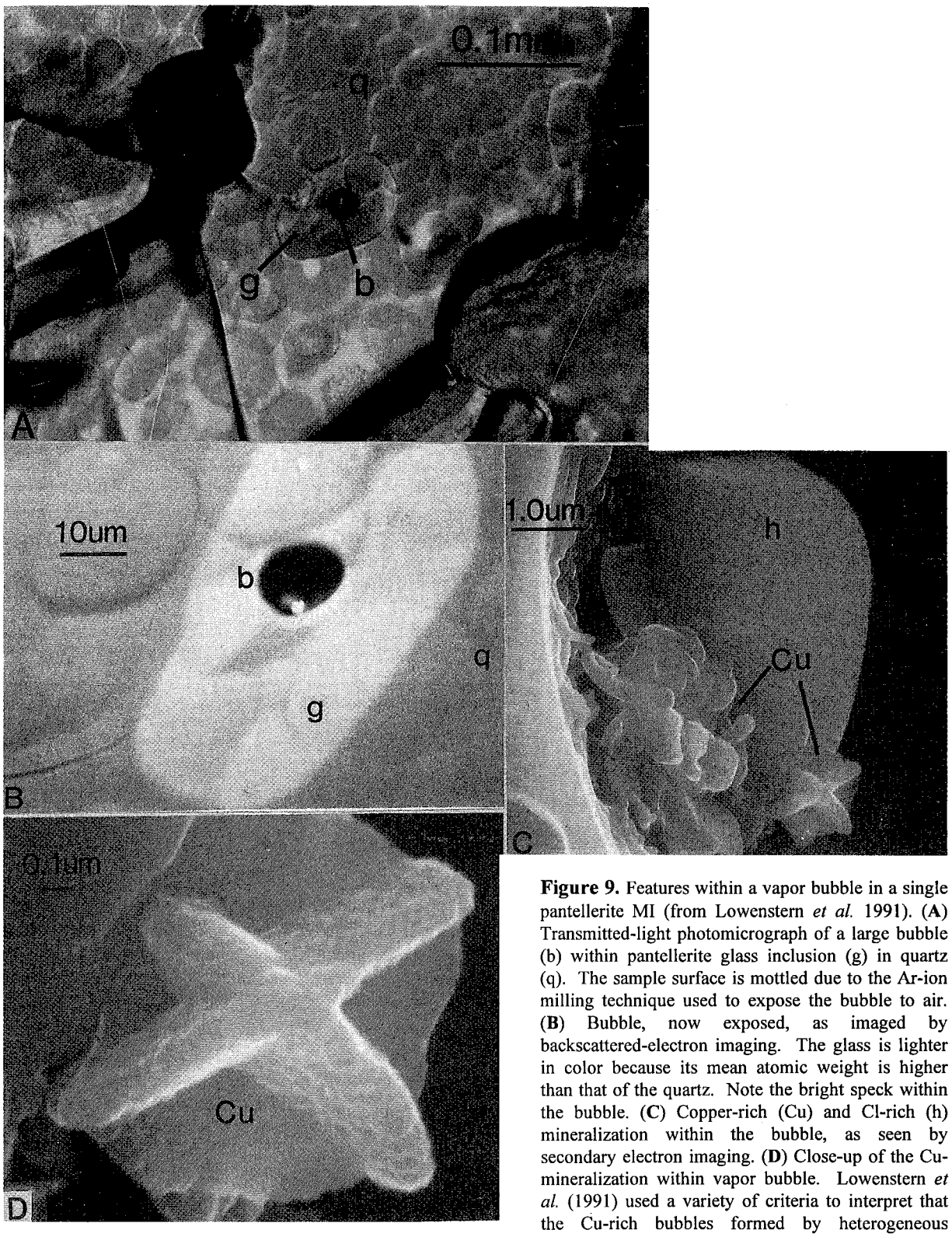

Figure 9. Features within a vapor bubble in a single pantellerite MI (from Lowenstern *et al.* 1991). (**A**) Transmitted-light photomicrograph of a large bubble (b) within pantellerite glass inclusion (g) in quartz (q). The sample surface is mottled due to the Ar-ion milling technique used to expose the bubble to air. (**B**) Bubble, now exposed, as imaged by backscattered-electron imaging. The glass is lighter in color because its mean atomic weight is higher than that of the quartz. Note the bright speck within the bubble. (**C**) Copper-rich (Cu) and Cl-rich (h) mineralization within the bubble, as seen by secondary electron imaging. (**D**) Close-up of the Cu-mineralization within vapor bubble. Lowenstern *et al.* (1991) used a variety of criteria to interpret that the Cu-rich bubbles formed by heterogeneous entrapment of pantellerite melt and a Cu-bearing volatile phase (see text).

PETROLOGIC AND STRATIGRAPHIC STUDIES

Silicate MI can record a variety of magmatic processes that control the evolution of igneous systems. The following subsections briefly list relevant tools and techniques (and appropriate references) that have been used to study mixing, crystallization, and other phenomena of interest to workers undertaking a study of a magma–hydrothermal system.

Magma Mixing and Crystal Fractionation

Silicate MI may be useful indicators of magma mixing, particularly when a rock has undergone some alteration or extensive crystallization of the groundmass. Under such circumstances, the MI may remain as reliable indicators of melt compositions during magmatic crystallization. Hervig & Dunbar (1992) studied both the Bishop and Bandelier magmatic systems, and used MI as evidence that magma mixing was an important process in producing the zonation within both of these magma bodies. The Hervig & Dunbar data for MI of the Lower Bandelier Tuff, plotted in Figure 10, can be divided into two groups. Matrix glass plots within the less differentiated group; this is inconsistent with crystal fractionation, wherein the matrix should represent the most differentiated composition. The data were interpreted to indicate mixing between low- and high-Ti melts. In earlier studies, Anderson (1976) and Rhodes *et al.* (1979) used MI as evidence for mixing events during the formation of andesitic magmas and ocean-floor basalts, respectively. Halsor (1989) studied large clear MI within plagioclase from andesites erupted at Toliman volcano in Guatemala. He concluded that MI were not in equilibrium with either bulk rock or matrix liquid, and that a mixing event caused rapid growth of the plagioclase and entrapment of large MI.

Crystallization and fractionation may be recorded by the compositions of a suite of MI trapped at different times. As opposed to mixing trends, which are linear on trace-element scatter plots, crystallization will result in data trends that are curved for compatible elements. Differentiation may be observed by analysis of MI within a single crystal or a group of phenocrysts. Lu *et al.* (1992) used trace-element concentrations in MI to calculate the amount of crystal fractionation during crystallization of the Bishop Tuff magma. Vaggelli *et al.* (1993) used changes in MI

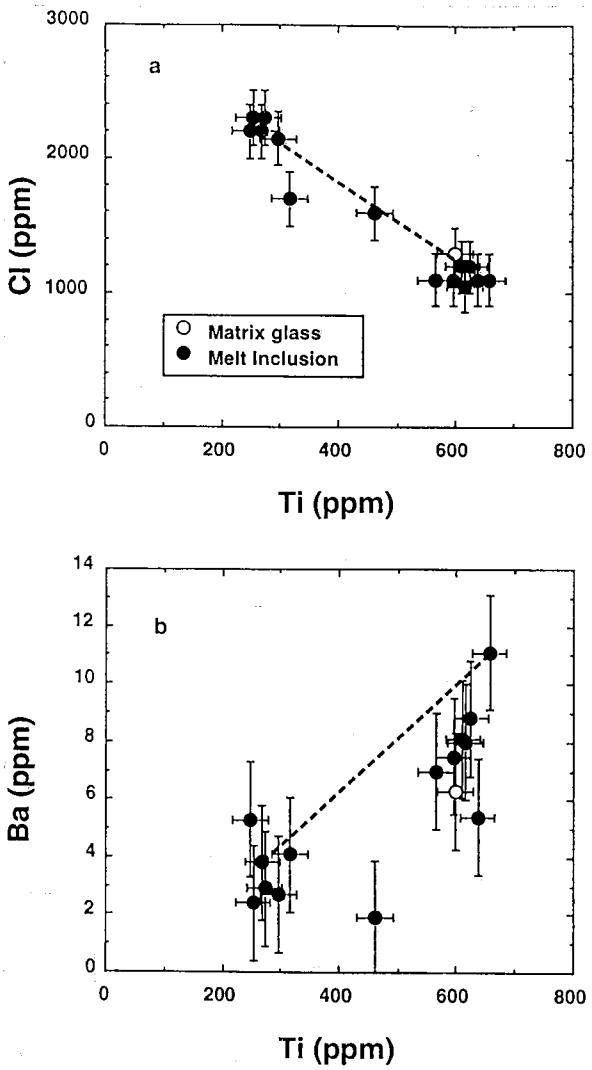

Figure 10. Variation of the compositions of melt inclusions (filled dots) from sample 030 from a pumice lump in the ignimbrite of the Lower Bandelier Tuff. The open circle represents matrix glass and the dashed line connects two inclusions in the same quartz phenocryst. (**a**) Variation of Ti with Cl. (**b**) Variation of Ti with Ba. "Bulk" denotes the composition of the bulk magma. The plots are consistent with mixing between high-Ti and low-Ti melts. The matrix glass plots within the less differentiated group, which would be unexpected if the trend in melt compositions were caused by fractionation of crystals. From Hervig & Dunbar (1992).

compositions between cores and rims of clinopyroxene crystals as evidence for crystal fractionation in recent Vesuvius lavas.

Experimental Petrology

Because MI approach constant-volume closed systems, they can be used as experimental pressure vessels for high-temperature petrological experiments. In effect, most homogenization experiments are exercises in experimental petrology. Pressure in the inclusion is a function of temperature (Fig. 4) and can be varied by means of a heating stage or furnace. Ideally, one can determine the solidus and liquidus of magmas by heating naturally crystallized inclusions. Clocchiatti & Massare (1985) used silicate MI within plagioclase as experimental vessels that they could monitor as a function of equilibration temperature. By doing experiments at different temperatures on separate groups of MI, they were able to replicate melt and phenocryst compositions obtained with high-pressure experimental apparatuses on similar tholeiite compositions. Roedder (1976) presented similar thermometric data on MI from lunar and Hawaiian basalts, though without EPMA analyses of the "run-products". Roedder (1972) performed laboratory experiments on MI to estimate magmatic conditions during formation of Ascension Island trachytes.

Stratigraphic Correlations

One of the most recent uses of MI has been the correlation of tonsteins (bentonitized ash-beds) within ancient lithologic sequences. Because the volcanic ash has been completely altered to clay, whole-rock compositions and glass-shard compositions cannot be used for stratigraphic correlations. However, Delano *et al.* (1994) were able to use MI to differentiate a variety of individual units and to define regional-scale stratigraphic time-planes; even though Ordovician rocks were studied, the inclusions were still glassy and seemingly unaltered. Economic geologists can use MI to define the stratigraphy of mineralized terranes and to correlate units in highly altered areas. Potentially, MI can be used to study the mass balance of bentonite-style (or any other kind of) alteration or to characterize the volatile concentrations in ancient eruptive sequences (Webster *et al.* 1995).

MELT INCLUSIONS IN GRANITES AND XENOLITHIC EJECTA

For the most part, MI are absent in granitic rocks because the prolonged cooling history of these rocks allows complete crystallization of the inclusions, erasing any record of their existence (Tuttle 1952). Only in rapidly cooled intrusions will MI remain intact and unaltered. In the ~280-Ma Mount Genis granite in southeastern Sardinia, Frezzotti (1992) found MI (some glassy) within equigranular granites as well as in crystals lining miarolitic cavities. Coexisting brine was interpreted as having formed during the late stages of crystallization of the magma. The MI were analyzed by EPMA, and several contained typical high-silica rhyolite glass with Cl concentrations reflecting equilibrium with vapor and hydrosaline melt (Shinohara 1994). Hansteen & Lustenhouwer (1990) examined MI and coexisting aqueous inclusions from the Permian Eikeren-Skrim granite in Norway. The inclusions homogenized at 685-705 °C, were composed of rhyolitic and rhyodacitic glass (not peralkaline), and were trapped at the same time as a saline aqueous fluid. Eadington & Nashar (1978) described and analyzed glass inclusions from topaz-quartz rocks from the New England district of New South Wales in Australia. Many of the MI contained several wt.% F, as well as apparent high H_2O concentrations. Weisbrod (1981) reviewed several studies of coexisting fluid and melt inclusions in shallow intrusions and porphyry deposits. Takenouchi & Imai (1975) described MI from a variety of porphyry and volcanic rocks and observed the effects of cooling history on the characteristics of MI.

Occasionally, intrusive rocks are ejected as xenoliths during volcanic eruptions. Studies of such samples have often resulted in discovery of CO_2-rich fluids in equilibrium with melt in the environment in which the xenoliths grew (Roedder 1965; Belkin *et al.* 1985; Frezzotti *et al.* 1991; Belkin & De Vivo 1993). Other xenoliths show evidence for immiscibility between silicate melt and hypersaline fluids (Roedder & Coombs

1967) or entrapment of both phases, though at different times (De Vivo *et al.* 1993).

SUMMARY

Silicate MI contain information on the dissolved volatile concentrations in igneous rocks (Tables 2 and 3). A variety of analytical and thermometric methods can be used to extract information from MI, as regards magmatic volatile concentrations, the compositions of exsolved magmatic fluids, and the pressure and temperature conditions under which magmas undergo crystallization. New techniques promise to increase the number of possible uses of MI, lengthening the first half of Table 1 and shortening its last half. For example, given improving microbeam techniques, MI may contribute new data on the stable-isotopic (H, O, S, Cl) composition of non-degassed magmas, and on what effect degassing has on the isotopic composition of silicate melt. New microbeam dating methods may allow assessment of the time delay between crystallization (MI formation) and eruption. Combined with the ever-increasing data-set on volatile solubilities, MI may yield more reliable estimates of the depths to magma chambers than are currently available through mineral geobarometers. As such, analysis of MI is likely to remain one of the most useful and reliable methods for understanding the behavior of volatile components in igneous systems, and MI will continue to provide insights for economic geologists, volcanologists, and other geoscientists.

ACKNOWLEDGEMENTS

Discussions over the past seven years have helped me to clarify my thinking about MI; I thank A.T. Anderson, C.R. Bacon, D.K. Bird, P. Fiske, G.A. Mahood, S. Newman, E. Roedder, H. Shinohara, T. Sisson, J. Stebbins, and P.J. Wallace for their input. The rest of my education about MI has been the legacy of excellent papers by A.T. Anderson, E. Roedder, R. Clocchiatti, and others, as well as the interesting samples I have had the good fortune to study. I appreciate reviews of the manuscript and helpful comments by C. Bacon, K. Bargar, H. Belkin, B. Bodnar, J. Hedenquist, H. Shinohara, and S. Simmons.

REFERENCES

AINES, R.D., LOWENSTERN, J.B. & MAHOOD, G.A. (1990): Evidence for CO_2-rich vapor in pantellerite magma chambers. *EOS, Trans. Am. Geophys. Union* **71**(43), 1699.

ANDERSON, A.J. & BODNAR, R.J. (1993): An adaption of the spindle stage for geometric analysis of fluid inclusions. *Am. Mineral.* **78**, 657-664.

ANDERSON, A.T., JR. (1974a): Evidence for a picritic, volatile-rich magma beneath Mt. Shasta, California. *J. Petrology* **15**, 243-267.

ANDERSON, A.T., JR. (1974b): Chlorine, sulfur and water in magmas and oceans. *Geol. Soc. Am. Bull.* **85**, 1485-1492.

ANDERSON, A.T., JR. (1976): Magma mixing: Petrological process and volcanological tool. *J. Volcanol. Geotherm. Research* **1**, 3-33.

ANDERSON, A.T., JR. (1991): Hourglass inclusions: Theory and application to the Bishop rhyolitic Tuff. *Am. Mineral.* **76**, 530-547.

ANDERSON, A.T., JR. & BROWN, G.G. (1993): CO_2 contents and formation pressures of some Kilauean melt inclusions. *Am. Mineral.* **78**, 794-803.

ANDERSON, A.T., JR., NEWMAN, S., WILLIAMS, S.N., DRUITT, T.H., SKIRIUS, C. & STOLPER, E. (1989): H_2O, CO_2, Cl and gas in Plinian and ash flow Bishop rhyolite. *Geology* **17**, 221-225.

BACON, C.R. (1989): Crystallization of accessory phases in magmas by local saturation adjacent to phenocrysts. *Geochim. Cosmochim. Acta* **53**, 1055-1066.

BACON, C.R., NEWMAN, S. & STOLPER, E. (1992): Water, CO_2, Cl, and F in melt inclusions in phenocrysts from three Holocene explosive eruptions, Crater Lake, Oregon. *Am. Mineral.* **77**, 1021-1030.

BEDDOE-STEPHENS, B., ASPDEN, J.S. & SHEPHERD, T.J. (1983): Glass inclusions and

melt compositions of the Toba Tuffs, northern Sumatra. *Contrib. Mineral. Petrology* **83**, 278-287.

BELKIN, H.E. (1994): Microthermometric investigation: Th and Tm. Practical and theoretical aspects. *In* Fluid Inclusions in Minerals: Methods and Applications (B. De Vivo & M.L. Frezzotti, eds.). Blacksburg, Virginia, 7-24.

BELKIN, H.E. & DE VIVO, B. (1993): Fluid inclusion studies of ejected nodules from plinian eruptions of Mt. Somma-Vesuvius. *J. Volcanol. Geotherm. Research* **58**, 89-100.

BELKIN, H.E., DE VIVO, B., ROEDDER, E. & CORTINI, M. (1985): Fluid inclusions geobarometry from ejected Mt. Somma–Vesuvius nodules. *Am. Mineral.* **70**, 288-303.

BOGAARD, P.V.D. & SCHIRNICK, C. (1994): Single crystal laser $^{40}Ar/^{39}Ar$ ages of quartz protocrysts in the 0.761 Ma Bishop Tuff rhyolite (Long Valley, U.S.A.). *Trans. ICOG*, p. 32.

CLOCCHIATTI, R. (1975): Les inclusions vitreuses des cristaux de quartz. Étude optique, thermo-optique et chimique. Applications géologiques. *Mémoire. Soc. Géol.*, France, LIV, **122**, 1-96.

CLOCCHIATTI, R. & MASSARE, D. (1985): Experimental crystal growth in glass inclusions: the possibilities and limits of the method. *Contrib. Mineral. Petrology* **89**, 193-204.

CLOCCHIATTI, R., MASSARE, D. METRICH, N., JORON, J.L. & WEISS, J. (1990): Glass inclusions in quartz of pumice of Montagna Grande (Pantelleria, Island): Appropriate experimental systems for the study of the physico-chemical properties of hyperalkaline magmas. *13th Conference on Earth Sciences, Abstracts,* Grenoble, 31 (in French).

CZAMANSKE, G.K., SISSON, T.W., CAMPBELL, J.L. & TEESDALE, W.J. (1993): Micro-PIXE analysis of silicate reference standards. *Am. Mineral.* **78**, 893-903.

DELANO, J.W., TICE, S.J., MITCHELL, C.E. & GOLDMAN, D. (1994): Rhyolitic glass in Ordovician K-bentonites: A new stratigraphic tool. *Geology* **22**, 115-118.

DE VIVO, B. & FREZZOTTI, M.L. (1994): Evidence for magmatic immiscibility in Italian subvolcanic systems. *In* Fluid Inclusions in Minerals: Methods and Applications (B. De Vivo & M.L. Frezzotti, eds.). Blacksburg, Virginia, 345-362.

DE VIVO, B., FREZZOTTI, M.L. & LIMA, A. (1993): Immiscibility in magmatic differentiation and fluid evolution in granitoid xenoliths at Pantelleria: Fluid inclusions evidence. *Acta Vulcanologica* **3**, 195-202.

DUNBAR, N.W. & HERVIG, R.L. (1992a): Volatile and trace element composition of melt inclusions from the Lower Bandelier Tuff: Implications for magma chamber processes and eruptive style. *J. Geophys. Research* **97**, 15151-15170.

DUNBAR, N.W. & HERVIG, R.L. (1992b): Petrogenesis and volatile stratigraphy of the Bishop Tuff: Evidence from melt inclusions analysis. *J. Geophys. Research* **97**, 15129-15150.

DUNBAR, N.W., HERVIG, R.L. & KYLE, P.R. (1989): Determination of pre-eruptive H_2O, F and Cl contents of silicic magmas using melt inclusions: examples from Taupo volcanic center, New Zealand. *Bull. Volcanol.* **51**, 177-184.

EADINGTON, P.J. & NASHAR, B. (1978): Evidence for the magmatic origin of quartz topaz rocks from the New England Batholith, Australia. *Contrib. Mineral. Petrology* **67**, 433-438.

FREZZOTTI, M.L. (1992): Magmatic immiscibility and fluid phase evolution in the Mount Genis granite (southeastern Sardinia, Italy). *Geochim. Cosmochim. Acta* **56**, 21-33.

FREZZOTTI, M.L., DE VIVO, B. & CLOCCHIATTI, R. (1991): Melt–mineral fluid interactions in ultramafic nodules from alkaline lavas of Mount Etna (Sicily, Italy): melt and fluid inclusion evidence. *J. Volcanol. Geotherm. Research* **47**, 209-219.

GERLACH, T.M. & MCGEE, K.A. (1994): Total sulfur dioxide emissions and pre-eruption vapor-saturated magma at Mount St. Helens, 1980-88. *Geophys. Research Lett.* **21**, 2833-2836.

GERLACH, T.M., MCGEE, K.A., WESTRICH, H.R. & SYMONDS, R.B. (Accepted): Pre-eruption vapor saturation in magma of the climactic Mount

Pinatubo eruption: Source of the giant stratospheric sulfur dioxide cloud. *U.S. Geol. Survey. Prof. Paper.*

GERLACH, T.M., MCGEE, K.A. CASADEVALL, T.J. & FINNEGAN, D.L. (1994): Vapor saturation and accumulation in magmas of the 1989-1990 eruption of Redoubt volcano, Alaska. *J. Volcanol. Geotherm. Research* **62**, 317-337.

GUTMANN, J.T. (1974): Tubular voids within labradorite phenocrysts from Sonora, Mexico. *Am. Mineral.* **59**, 666-672.

HALL, D.L., BODNAR, R.J. & CRAIG, J.R. (1991): Evidence for postentrapment diffusion of hydrogen into peak metamorphic fluid inclusions from the massive sulfide deposits at Ducktown, Tennessee. *Am. Mineral.* **76**, 1344-1355.

HALSOR, S.P. (1989): Large glass inclusions in plagioclase phenocrysts and their bearing on the origin of mixed andesitic lavas at Tolimán Volcano, Guatemala. *Bull. Volcanol.* **51**, 271-280.

HANSTEEN, T.H. & LUSTENHOUWER, W.J. (1990): Silicate melt inclusions from a mildly peralkaline granite in the Oslo paleorift, Norway. *Mineral Mag.* **54**, 195-205.

HERVIG, R.L. & DUNBAR, N.W. (1992): Cause of chemical zoning in the Bishop (California) and Bandelier (New Mexico) magma chambers. *Earth Planet. Sci. Lett.* **111**, 97-108.

HERVIG, R.L., DUNBAR, N.W, WESTRICH, H.R. & KYLE, P. (1989): Pre-eruptive water content of rhyolitic magmas as determined by ion microprobe analyses of melt inclusions in phenocrysts. *J. Volcanol. Geotherm. Research* **36**, 293-302.

HOLLISTER, L.S. & CRAWFORD, M.L. (editors) (1982) Fluid Inclusions: Applications to Petrology. *Mineral. Assoc. Canada Short Course Vol.* **6**, 304 p.

HOLLOWAY, J.R. & BLANK, J.G. (1994): Application of experimental results to C-O-H species in natural melts. *Reviews Mineral.* **30**, 187-230.

IHINGER, P.D., HERVIG, R.L. & MCMILLAN, P.F. (1994): Analytical methods for volatiles in glasses. *Reviews Mineral.* **30**, 67-121.

JOHNSON, M.C., ANDERSON, A.T., JR. & RUTHERFORD, M.J. (1994): Pre-eruptive volatile contents of magmas. *Reviews Mineral.* **30**, 281-330.

KEITH, J.D. & SHANKS, W.C., III (1988): Chemical evolution and volatile fugacities of the Pine Grove porphyry molybdenum and ash-flow tuff system, southwestern Utah. *In* Recent Advances in the Geology of Granite-related Mineral Deposits (D.F. Strong & R.P. Taylor, eds.). *CIM Special Vol.* **39**, 402-423.

KEITH, J.D., SHANKS, W.C., III, ARCHIBALD, D.A. & FARAR, E. (1986): Volcanic and intrusive history of the Pine Grove porphyry molybdenum system, southwestern Utah. *Econ. Geol.* **81**, 553-577.

KOVALENKO, V.I., NAUMOV, V.B. & SOLOVOVA, I.P. (1993): Behavior of Cl during differentiation and eruption of magmas at Pantelleria. *Geochem. Internat.* **30**, 105-108.

KOVALENKO, V.I., NAUMOV, V.B., SOLOVOVA, I.P. GIRNIS, A.V., HERVIG, R.L. & BORIANI, A. (1994): Volatile components, composition, and crystallization conditions of the Pantelleria basalt - pantellerite association magmas, inferred from the melt and fluid inclusion data. *Petrology* **2**, 24-42 (translated from original Russian).

LAYNE, G.D. & STIX, J. (1991): Volatile and light lithophile element (LLE) evolution of the Jemez Mountains magmatic system I. The interval between caldera formation at 1.51 Ma and 1.14 Ma. *EOS, Trans. Am. Geophys. Union* **72**, 577.

LAYNE, G.D., STIX, J., WILLIAMS, S.N. (1992): Pre-eruptive concentrations of magmatic volatiles for the 13 November 1985 eruption of Nevado del Ruiz, Colombia. *EOS, Trans. Am. Geophys. Union* **73**, 367.

LEMMLEIN (1930): Corrosion and regeneration of quartz phenocrysts in quartz porphyries. *Doklady Akad. Nauk SSSR* **A-3**, 341-344.

LI, Z. (1994): The silicate melt inclusions in igneous rocks. *In* Fluid Inclusions in Minerals: Methods and Applications (B. De Vivo & M.L. Frezzotti, eds.). Blacksburg, Virginia, 73-94.

LOWENSTERN, J.B. (1993): Evidence for a copper-bearing fluid in magma erupted at the Valley of Ten Thousand Smokes, Alaska. *Contrib. Mineral. Petrology* **114**, 409-421.

LOWENSTERN, J.B. (1994a): Chlorine, fluid immiscibility, and degassing in peralkaline magmas from Pantelleria, Italy. *Am. Mineral.* **79**, 353-369.

LOWENSTERN, J.B. (1994b): Dissolved volatile concentrations in an ore-forming magma. *Geology* **22**, 893-896.

LOWENSTERN, J.B. & MAHOOD, G.A. (1991): New data on magmatic H_2O contents of pantellerites, with implications for petrogenesis and eruptive dynamics at Pantelleria. *Bull. Volcanol.* **54**, 78-83.

LOWENSTERN, J.B., MAHOOD, G.A., RIVERS, M.L. & SUTTON, S.R. (1991): Evidence for extreme partitioning of copper into a magmatic vapor phase. *Science* **252**, 1405-1409.

LU, F.Q., ANDERSON, A.T. & DAVIS, A.M. (1992) Melt inclusions and crystal-liquid separation in rhyolitic magma of the Bishop Tuff. *Contrib. Mineral. Petrology* **110**, 113-120.

LU, F.Q., SMITH, J.V., SUTTON, S.R., RIVERS, M.L. & DAVIS, A.M. (1989): Synchrotron X-ray fluorescence analysis of rock-forming minerals: 1) Comparison with other techniques 2) White-beam energy-dispersive procedure for feldspars. *Chem. Geol.* **75**, 123-143.

LUHR, J.F. (1990): Experimental phase relations of water- and sulfur-saturated arc magmas and the 1982 eruptions of El Chichón Volcano. *J. Petrology* **31**, 1071-1114.

MACLELLAN, H.E. & TREMBATH, L.T. (1991): The role of quartz crystallization in the development and preservation of igneous texture in granitic rocks: Experimental evidence at 1 kbar. *Am. Mineral.* **76**, 1291-1305.

MANLEY, C.R. (1994*): On Voluminous Rhyolite Lava Flows.* Ph.D. thesis, Arizona State University, Tempe, Arizona.

MAVROGENES, J.A. & BODNAR, R.J. (1994): Hydrogen movement into and out of fluid inclusions in quartz: Experimental evidence and geologic implications. *Geochim. Cosmochim. Acta* **58**, 141-148.

METRICH, N. & CLOCCHIATTI, R. (1989): Melt inclusion investigation of the volatile behavior in historic alkali basaltic magmas of Etna. *Bull. Volcanol.* **51**, 185-198.

MOSBAH, M., CLOCCHIATTI, R., TIRIRA, J., GOSSET, J., MASSIOT, P. & TROCELLIER, P. (1991) Study of hydrogen in melt inclusions trapped in quartz with a nuclear microprobe. *Nucl. Instrum. Methods* **54**, 298-303.

NASH, W.P. (1992): Analysis of oxygen with the electron microprobe: Applications to hydrated glass and minerals. *Am. Mineral.* **77**, 453-457.

NAUMOV, V.B., SOLOVOVA, I.P., KOVALENKER, V.A., RUSINOV, V.L. & KONONKOVA, N.N. (1991): First data on high-density fluid inclusions of magmatic water in phenocrysts in rhyolite. *Doklady Akad. Nauk SSSR* **318**, 187-190.

NEWMAN, S. & CHESNER, C. (1989): Volatile compositions of glass inclusions from the 75 Ka Toba Tuff, Sumatra. *Geol. Soc. Am. Abstr. Programs* **21**, 271.

NIELSEN, C.H. & SIGURDSSON, H. (1981): Quantitative methods for electron microprobe analysis of sodium in natural and synthetic glasses. *Am. Mineral.* **66**, 547-552.

PALAIS, J. & SIGURDSSON, H. (1989): Petrologic evidence of volcanic emissions from major historic and prehistoric eruptions. *In* Understanding Climate Change (A. Berger, R. Dickenson & J.W. Kidson, eds.). *Am. Geophys. Union Geophys. Monogr.* **52**, 31-53.

PASTERIS, J.D. & WANAMAKER, B.J. (1988): Laser Raman microprobe analysis of experimentally re-equilibrated fluid inclusions in olivine: Some implications for mantle fluids. *Am. Mineral.* **73**, 1074-1088.

PASTERIS, J.D., WANAMAKER, B.J., WOPENKA, B., WANG, A. & HARRIS, T.N. (accepted): Relative timing of fluid and anhydrite saturation: Another consideration in the sulfur budget of the Mount Pinatubo eruption. *U.S. Geol. Surv. Prof. Paper.*

QIN, Z. (1994): *Melting and Diffusive Equilibration in Igneous Processes*. Ph.D. thesis, Univ. Chicago, Chicago, Illinois.

QIN, Z., LU, F. & ANDERSON, A.T., JR. (1992): Diffusive reequilibration of melt and fluid inclusions. *Am. Mineral.* **77**, 565-576.

RHODES, J.M., DUNGAN, M.A., BLANCHARD, D.P. & LONG, P.E. (1979): Magma mixing at mid-ocean ridges: Evidence from basalts drilled near 22°N on the Mid-Atlantic Ridge. *Tectonophysics* **55**, 35-61.

ROEDDER, E. (1965): Liquid CO_2 inclusions in olivine-bearing nodules and phenocrysts from basalts. *Am. Mineral.* **50**, 1746-1782.

ROEDDER, E. (1972): Laboratory studies on inclusions in minerals of Ascension Island granitic blocks, and their petrologic significance. *Proceedings of COFFI* **5**, 129-138.

ROEDDER, E. (1976): Petrologic data from experimental studies on crystallized silicate melt and other inclusions in lunar and Hawaiian olivine. *Am. Mineral.* **61**, 684-690.

ROEDDER, E. (1979): Origin and significance of magmatic inclusions. *Bull. Mineral.* **102**, 487-510.

ROEDDER, E. (1984): Fluid Inclusions. *Reviews Mineral.* **12**, 644 p.

ROEDDER, E. (1992): Fluid inclusion evidence for immiscibility in magmatic differentiation. *Geochim. Cosmochim. Acta* **56**, 5-20.

ROEDDER, E. & COOMBS, D.S. (1967): Immiscibility in granitic melts, indicated by fluid inclusions in ejected granitic blocks from Ascension Island. *J. Petrology* **8**, 417-451.

ROGGENSACK, K., WILLIAMS, S.N. & HERVIG, R.L. (1993): Melt inclusion water contents within the 1902 eruption of Santa Maria Volcano, Guatemala. *EOS, Trans. Am. Geophys. Union* **74**, 621.

RUTHERFORD, M.J., SIGURDSSON, H., CAREY S. & DAVIS, A. (1985): The May 18, 1980 eruption of Mount St. Helens, 1. Melt composition and experimental phase equilibria, *J. Geophys. Research* **90**, 2929-2947.

SCHIANO, P., CLOCCHIATTI, R., SHIMIZU, N., WEIS, D. & MATTIELLI, N. (1994): Cogenetic silica-rich and carbonate-rich melts trapped in mantle minerals in Kerguelen ultramafic xenoliths: Implications for metasomatism in the oceanic upper mantle. *Earth Planet. Sci. Lett.* **123**, 167-178.

SCOWEN, P.A.H., ROEDER, P.L. & HELZ, R.T. (1991): Reequilibration of chromite within Kilauea Iki lava lake, Hawaii. *Contrib Mineral. Petrology* **107**, 8-20.

SHINOHARA, H. (1994): Exsolution of immiscible vapor and liquid phases from a crystallizing silicate melt: Implications for chlorine and metal transport. *Geochim. Cosmochim. Acta* **58**, 5215-5221.

SISSON, T.W. & LAYNE, G.D. (1993): H_2O in basalt and basaltic andesite glass inclusions from four subduction-related volcanoes. *Earth Planet. Sci. Lett.* **117**, 619-635.

SKIRIUS, C.M. (1990): *Pre-eruptive H_2O and CO_2 Content of Plinian and Ash-flow Bishop Tuff Magma*. Ph.D. thesis, Univ. Chicago, Chicago, Illinois.

SKIRIUS, C.M., PETERSON, J.W. & ANDERSON, A.T., JR. (1990): Homogenizing rhyolitic glass inclusions from the Bishop Tuff. *Am. Mineral.* **75**, 1381-1398.

SOBOLEV, V.S. & KOSTYUK, V.P. (1975): Magmatic crystallization based on a study of melt inclusions. *Fluid Inclusion Research* **9**, 182-253 (translated from original publication in Russian).

SOLOVOVA, I., NAUMOV, V., GIRNIS, A., KOVALENKO V. & GUZHOVA, A. (1991): High-temperature fluid heterogeneity: Evidences from microinclusions in Pantelleria volcanics. *Plinius* **5**, 206.

SORBY, H.C. (1858): On the microscopical structure of crystals, indicating the origin of minerals and rocks. *Quart. J. Geol. Soc. London* **14**, 453-500.

STIX, J., ZAPATA, J.A., CALVACHE, M., CORTÉS, G.P., FISCHER, T.P., GÓMEZ, D., NARVAEZ, L., ORDOÑEZ, M., ORTEGA, A., TORRES, R. & WILLIAMS, S.N. (1993): A model of degassing at Galeras Volcano, Colombia, 1988-1993. *Geology*

21, 963-967.

SYMONDS, R.B., ROSE, W.I., BLUTH, G.J.S. & GERLACH, T.M. (1994): Volcanic-gas studies: Methods, results and applications. *Reviews Mineral.* **30**, 1-66.

TAIT, S. (1992): Selective preservation of melt inclusions in igneous phenocrysts. *Am. Mineral.* 77, 146-155.

TAKENOUCHI, S. & IMAI, H. (1975): Glass and fluid inclusions in acidic igneous rocks from some mining areas in Japan. *Econ. Geol.* **70**, 750-769.

TUTTLE, O.F. (1952): Origin of the contrasting mineralogy of extrusive and plutonic salic rocks. *J. Geol.* **60**, 107-124.

VAGGELLI, G., DE VIVO, B. & TRIGILA, R. (1993): Silicate-melt inclusions in recent Vesuvius lavas (1631-1944): II. Analytical chemistry. *J. Volcanol. Geotherm. Research.* **58**, 367-376.

WALLACE, P., ANDERSON, A.T. & DAVIS, A.M. (1994): Preeruptive gradients in H_2O, CO_2, and exsolved gas in the magma body of the Bishop tuff. *EOS, Trans. Am. Geophys. Union* **75**, 718.

WALLACE, P.J. & GERLACH T.M. (1994): Magmatic vapor source for sulfur dioxide released during volcanic eruptions: Evidence from Mount Pinatubo. *Science* **265**, 497-499.

WATSON, E. B. (1976): Glass inclusions as samples of early magmatic liquid: determinative method and application to a South Atlantic basalt. *J. Volcanol. Geotherm. Research.* **1**, 73-84.

WATSON, E. B., SNEERINGER, M.A. & ROSS, A. (1982): Diffusion of dissolved carbonate in magmas: experimental results and applications. *Earth Planet. Sci. Lett.* **61**, 346-358.

WEBSTER, J.D. & DUFFIELD, W.A. (1991): Volatiles and lithophile elements in Taylor Creek Rhyolite: Constraints from glass inclusion analysis. *Am. Mineral.* **76**, 1628-1645.

WEBSTER, J.D. & DUFFIELD, W.A. (1994): Extreme halogen abundances in tin-rich magma of the Taylor Creek rhyolite, New Mexico. *Econ. Geol.* **89**, 840-850.

WEBSTER, J.D., CONGDON, R.D. & LYONS, P.C. (1995): Determining pre-eruptive compositions of Late Paleozoic magma from kaolinized volcanic ashes: Analysis of glass inclusions in quartz microphenocrysts from tonsteins. *Geochim. Cosmochim. Acta* **59**, 711-720.

WEBSTER, J.D., TAYLOR, R.P. & BEAN, C. (1993): Pre-eruptive melt composition and constraints on degassing of a water-rich pantellerite magma, Fantale Volcano, Ethiopia. *Contrib. Mineral. Petrology* **114**, 53-62.

WEISBROD, A. (1981): Fluid inclusions in shallow intrusives. *In* Short Course in Fluid Inclusions: Applications to Petrology (L.S. Hollister & M.L. Crawford, eds.). *Mineral. Assoc. Can. Short Course Vol.* **6**, 241-271.

WESTRICH, H.R. & GERLACH, T.M. (1992): Magmatic gas source for the stratospheric SO_2 cloud from the June 15, 1991 eruption of Mount Pinatubo. *Geology* **20**, 867-870.

WESTRICH, H.R., EICHELBERGER, J.C. & HERVIG, R.L. (1991) Degassing of the 1912 Katmai magmas. *Geophys. Research Lett.* **18**, 1561-1564.

WILDING, M.C., MACDONALD, R., DAVIES, J.E. & FALLICK, A.E., (1993): Volatile characteristics of peralkaline rhyolites from Kenya: an ion microprobe, infrared spectroscopic and hydrogen isotope study. *Contrib. Mineral. Petrology* **114**, 264-275.